Acknowledgements

We would like to give a huge thank you to associate professor Johannes Jäschke for being our supervisor. You have been a great support, and helped us a lot. Thank you for your good guidance. You have also given us the freedom to make our own decisions, and to think for ourselves.

Thank you Gro Mogseth, for all your guidance according subsea equipment and practical issues. Also, we would send a thank you to Sigurd Skogestad for taking his time to answers our questions.

Abstract

The basis of this project was Case 2, from the SUBPRO Business Cases, ”Field Characteristics and Design Data”[24]. This case represents a remote, low energy oil field with low pressure, 90 bar, and low temperature, 26°C. The nearest facility is placed 150 km from the reservoir. Three designs were designed for subsea separation and water treatment over a period of 10 years, to reach the goal of discharging waste water directly into the seawater. Case 1, including two gravity separators, one hydrocyclone and one flotation unit was found to be the optimal case regarding robustness and adaptability.

The total CAPEX was estimated to be 485 669 379 USD, and the total OPEX was estimated to be 27 220 968. From the investment analysis, the NPV was estimated to be 658.27 mill. USD, and the pay-back time 3.12 years. From the sensitivity analysis, the break-even oil price was found to be approximately 28.14 USD/bbl.

Contents

List of Figures

List of Tables

1 Introduction

Rougher, deeper and more challenging oil fields have driven the growth of subsea activity. Subsea processing has the potential to revolutionise the traditional offshore oil and gas production. By improving mature subsea technology one can achieve reduced development cost, increase reservoir productivity and recovery[29].

Norway has been in the forefront of subsea development since the 1990s. New reservoirs had just been discovered around Statfjord field, but were to small to make individual production viable. When it was established that the subsea production was a realistic and realisable option, engineers began developing less complicated and cost-effective solutions[30]. This resulted in the possibility of making small reservoirs like the ones found around the Statfjord field financially viable. The goal was to create a fully operating subsea system integrated with existing infrastructure. During the late 1990s, several large international companies started taking interest in subsea solutions, and subsea production turned out to be beneficial for smaller fields that could not justify building and operation of large platforms[30].

However, the subsea industry is still facing many challenges. Deeper water, greater complexities and more complicated logistics makes it harder to seek new reservoirs to satisfy the worldwide demand. One important challenge, yet to be solved efficient, is subsea separation and treatment of produced water[7]. Strict disposal regulations and lack of reliable technology is why there has been no wider uptake of subsea separation systems[7].

This report studies the possibility of making a robust and adaptable subsea separation and water treatment system, and by adopting existing solutions, investigate whether the system is able to tackle strict regulations and cope with changing liquid flows to make a financially viable system.

2 Background

2.1 Subsea separation

Subsea separation is, by definition, a separation process where the entire system is moved to the seabed and the processed flows are sent to the topside[1]. There are several advantages with subsea separation. Moving the entire water treatment system subsea can reduce the cost related to the process of lifting the produced water topside. By reducing the amount of production transferred from the seabed to the surface, the topside capacity utilisation can be improved reducing both operating and capital costs.

In general, a subsea processing facility is robust and adaptable. As the subsea location constraints the possibility of physically maintenance, inspection and modifications, the facility needs to be able to cope with both expected and unexpected changes in flows and compositions[1]. All subsea equipment will be expensive and time-consuming to repair, retrieve or replace once installed. To reduce the risk of failure and ensure equipment reliability, testing and qualification are critical.

For deepwater solutions, small and compact separators with low residence time will often be more sensitive to changing operating conditions, but are more easily replaced with more suitable ones. In contrast, the large gravity separators are more adaptable to changing liquid and gas flows. However, gravity separators are not efficient enough to reach the disposal requirement alone[1].

2.2 Produced water treatment

To meet the disposal regulations required, the produced water must be treated for contamination of oil and solids. The purified water can either be used in a produced water reinjection(PWRI) process, or be discharged directly into the ocean[6].

For a produced water reinjection, the requirement are quite strict for both oil content and solids specifications. The oil content must be between 10-30 ppm. The solids size must to be between 5-10 microns with an oil content less than 5 ppm. The reason for these strict requirements for oil removal and solids removal is to prevent formation damage. To discharge the water into the ocean there are usually no specification for the solids, but the oil content has to be less than 30ppm[6].

To reach the disposal regulations, the produced water must be treated through several separation process steps. The initial separation is usually gross separation with gravity separators. For a topside facility, the second separation step can be separation with hydrocyclones, both desanders and deoilers. This is to remove the bulk of the solids and oil. Hydrocyclones can separate down to an oil content between 10-30 ppm, and to a 10 micron particle size of sand. In the third separation step it is common to perform a separation with induced gas flotation (IGF). If the disposal regulations still are not reached, a fourth separation step can be added. This separation can be with a nut shell media filtration (NSF)[6].

2.3 Challenges with subsea separation

Subsea separation is a relatively unexplored area with little previous experience to build upon[7]. In general, subsea conditions offer a much harsher environment, which makes it hard to adopt existing technologies. There are also limited qualification testing facilities for subsea separation[7]. Flow assurance, produced water treatment analysis and pressure limitations are also important considerations when installing a subsea water treatment system. Developing solutions to cope with all existing problems is out of this thesis scope, but will be presented as important aspects of subsea water treatment.

2.3.1 Flow assurance

To ensure that hydrocarbon reservoir fluids can be moved safe and economically to the refinery, with focus on the engineering discipline and the knowledge about fluid and the technology required, is called flow assurance[53]. Issues regarding sand handling, hydrate formation, wax deposition, asphaltenes, corrosion, erosion and scale deposition is just some of the considerations when it comes to flow assurance[54].

2.3.2 Sand management

Pumping oil from a reservoir will bring some sand with it, together with crude oil, water and gas. The composition of the well stream will vary between wells and the lifetime of the field. To cope with these variations a subsea processing system has to be able to adapt[1].

There are several challenges related to sand in subsea separation processes. Some of them can be degradation of pumps as a result of wear, clogging of separation equipment and erosion of pipelines[2]. Another problem caused by sand is that, due to a high density, the sand will settle to the bottom of the gravity-separator. This can form large layers of sand at the bottom of the separator, fill it up and change the performance of the separation[4].

Equipment used in sand handling are typically desanding hydrocyclones, cyclonic jetting systems or sand accumulator vessels. Removal of sand from the processing system can be routed in different ways. For example, in the Tordis field, the sand was re-injected with the water, and in the Pazflor field, Angola, the sand was transported to the surface together with the oil[2].

2.3.3 Produced water treatment analysis

For conventional topside separation systems the oil in water content is physically collected and analysed before the waste water gets discharged into the sea. Due to the practicalities around oil-in-water measurements without manually sampling and analysis, the procedure is inconvenient to perform subsea[1]. Presently there are no available instruments to continuously monitor the oil content for treated waste water subsea[7].

2.3.4 Pressure limitations

One of the challenges when installing the equipment on the seabed is to maintain the high seawater pressure. The pipelines and components used in the subsea design has to keep a pressure which is equal or greater than the external seawater pressure. This is to prevent equipment from imploding. The external seawater pressure can be calculated by,

$$P_{ext} = \rho g h \tag{1}$$

where ρ is the density of water, g is the gravity constant, and h is the depth of water. To sustain the high pressure in the equipment, the walls can be made thicker or it can be used a compensation system[9].

3 Separation and water treatment technology

3.1 Gravitational separator

The separation from a gravity separator is driven by the density differences in the phases and gravitational forces. The gravity separator can either be a two-phase separator or a three-phase separator. A two-phase separator typically has one gas outflow and one liquid outflow. While a three-phase separator typically has one gas outflow, one light liquid outflow and one heavy liquid outflow. The separator used for water treatment here is a three-phase separator and can either be designed as a horizontal or vertical pressure vessel. Because a long liquid hold-up time is required, a horizontal separator is selected. An illustration of a horizontal three-phase separator is shown in Figure 1.

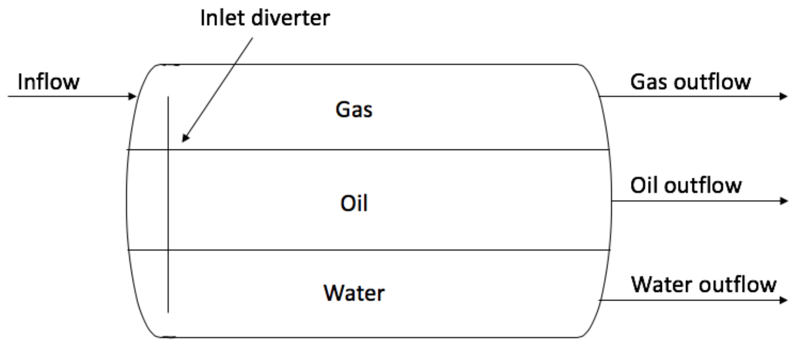

Figure 1: Horizontal three-phase gravity separator.

The three-phase separator is usually the first separator in a water treatment plant, and is used to separate the largest oil droplets from water. When the inflow enters the separator it hits an inlet diverter which will do the initial main separation of vapour and liquid. This is because of the sudden change in momentum. To direct the liquid flow below the oil-water interface, the inlet diverter will in most designs contain a downcomer. The mixture of oil and water will then be forced to mix with the water continuous phase in the bottom of the separator. Afterwards, the droplets can rise through the oil-water interface. This process leads to a better chance of coalescence of water droplets, and is called ”water-washing”. It will also assure that the liquid does not fall on top of the gas/oil interphase or the oil/water interphase. Because of the inlet diverter, the liquid flow will only carry a small part of gas to the bottom of the vessel[5].

3.2 Hydrocyclone

Hydrocyclones are widely used today because of the great efficiency, and can remove up to 90% of the incoming oil. The efficiency of hydrocyclones is dependent of the oil bubble distribution, and is usually only capable of separating oil droplets larger than 30 microns[17]. Hydrocyclones are therefore located upstream in the process.

A hydrocyclone is a device that utilize centrifugal force to promote separation of components with different densities. By directing the inflow tangentially at the top, the hydrocyclone gives the incoming liquid a rotary motion. As the entire content in the cyclone spins, this forces water, the heavy component, to move towards the wall. The light component, oil, forms a core in the centre and is pushed upwards and discharged through the top outlet, as shown in Figure 2.

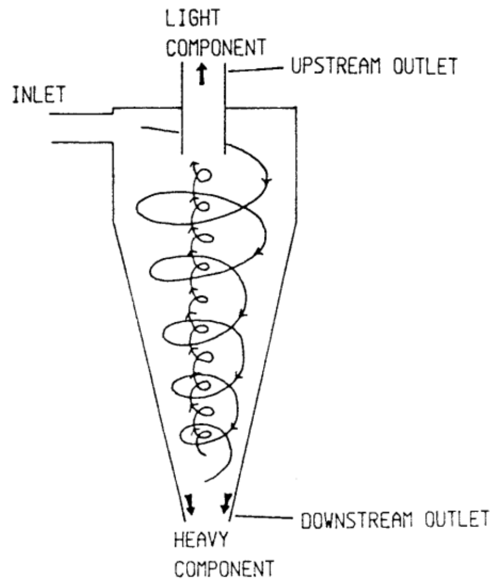

Figure 2: Illustration of the streamlines for heavy and light component in a hydrocyclone[17].

3.3 Gas Flotation

Gas flotation is a water treatment process that can be used to remove small oil droplets from the waste water stream by injecting gas. As the oil drops from the bulk flow moves down the tank they will collide with the gas stream as shown in Figure 3. When a collision occur the oil droplets will either attach or bounce off. If an oil bubble gets captured, it will rise with the gas to the surface of the tank creating an oily foam which can be removed. Since flotation units usually are capable of separating smaller oil drops, it is always located downstream of primary separators[20].

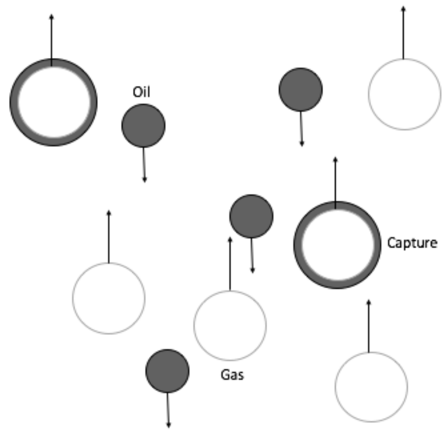

Figure 3: Principle of oil capture inside a flotation unit.

The two main flotation units relevant for deoiling purposes are induced gas flotation(IGF) and dissolved air flotation(DAF). Both IGF and DAF utilize the same working principles, but differs in the way the gas is injected and gas bubble size it produce. In the dissolved air flotation the gas is injected while the liquid is pressurised which typically produces gas bubbles in the range of 30-50 microns[40]. In the induced gas flotation units the gas is pumped directly in, saturating the waste water, producing gas bubbles from 70 microns and larger[40]. DAF is often considered to be more effective compared to IAF. However, IGF requires fewer parts which results in an overall smaller capital and maintenance cost. Due to the fact that the flotation unit will be located subsea which constraints the availability, induced gas flotation is therefore the best candidate for subsea flotation.

4 Design Basis

The basis of this project is Case 2, from the SUBPRO Business Cases, "Field Characteristics and Design Data"[24]. This case represents a remote, low energy oil field, with low pressure and temperature. The location is assumed to be nearby Norway, so that taxes and prices are according to Norwegian standard in 2018. It is assumed that an already existing oilfield is available, and this subsea separation system can be connected to the oilfield. As a result of this, there is no need for drilling wells, and already installed manifolds and subsea trees are used. The oil price[56] and the gas price[55] used in the calculations are retrieved 18.11.2018.

The properties for the oil field and the oil and gas prices are given in Table 1.

Table 1: Properties for the oil field, and oil and gas prices.

Description	Value	Unit
Reservoir pressure[24]	90	bar
Reservoir temperature[24]	26	°C
Reservoir depth[24]	400	m
Gas oil ratio[24]	100	$\frac{Sm^3}{Sm^3}$
Seabed water depth[24]	500	m
Seabed temperature[24]	4	°C
Oil price[56]	66.64	$\frac{USD}{bbl.}$
Gas price[55]	4.272	$\frac{USD}{Mmbtu}$

The properties for maximum oil production, maximum water production and maximum liquid production are given in Table 2[24].

Table 2: Properties for the production profiles: Maximum oil production, maximum water production and maximum liquid production.

Production profile	Value	Unit
Maximum oil production		
Oil production	7000	Sm^3/d
Water production	900	Sm^3/d
Maximum water production		
Oil production	400	Sm^3/d
Water production	8500	Sm^3/d
Maximum liquid production		
Oil production	6500	Sm^3/d
Water production	4600	Sm^3/d

The composition of the well stream, with corresponding molar weights, are given in Table 3[24].

Table 3: Composition of the well stream.

Component	Mole fraction [-]	Molar weight [g/mol]
N_2	0.00472	28.014
CO_2	0.0005	44.01
CH_4	0.3464	16.043
C_2H_6	0.03229	30.07
C_3H_8	0.2417	44.097
iC_4H_{10}	0.00554	58.124
nC_4H_{10}	0.0167	58.124
$iso - C_5H_{12}$	0.00019	72.151
iC_5H_{12}	0.00546	72.151
nC_5H_{12}	0.00684	72.151
C_6H_{14}	0.00992	85.3
C_7H_{16}	0.0169	92.7
C_8H_{18}	0.0217	105.8
C_9H_{20}	0.0174	121.7
$C_{10}+$	0.4964	271

It is assumed that N_2, CO_2 and CH_4 are the only compounds that constitutes the gas phase. The oil is assumed to be light crude oil, which is defined by having a density that is equal or less than 870 kg/m^3[23]. The densities used in the simulations are given in Table 4.

Table 4: Densities used in the simulations at normal temperature and pressure (NTP).

Compound	Density [kg/m^3]
N_2 [21]	1.165
CO_2 [21]	1.842
CH_4 [21]	0.668
H_2O	998
Light crude oil [23]	870

4.1 Gravity separator

The gravity separator was modelled in Matlab based on an empirical formula with a user specified efficiency, and simulated in Matlab. The model is presented in Appendix A.1.

4.1.1 Model assumptions

The following assumptions were made to simulate the three-phase separator.

- The efficiency can be calculated by an empirical formula.
- The gas phase does not occupy any volume.
- The gravity separator is modelled as a two phase separator with oil and water.
- Perfect gas-liquid separation.
- An ideal homogeneous mixture of oil- and water-flows.

4.1.2 Design parameters

The separator dimensions, wall thickness and cost calculations used in the model are shown in Table 5. A complementary calculation procedure for the dimensions are shown in Appendix B.1.

Table 5: Three-phase gravity separator dimensions.

Dimension	Value	Unit
D_v	1.47	m
L_v	7.34	m
V_v	12.42	m^3
t_w	60	mm

4.2 Hydrocyclone

The hydrocyclone was simulated in Matlab using empirical formulas based on experimental values[17]. Since the efficiency is only valid for a certain range of oil droplet sizes a distribution was established. The model is presented in Appendix A.2.

4.2.1 Model assumptions

The following assumptions were made to simulate the hydrocyclone.

- The separation efficiency can be calculated using an empirical model based on experimental values.
- Inlet oil droplet distribution is normal distributed and with radius ranging from 1 to 150 mm.
- Inlet volumetric flow rate can be calculated by dividing the total flow rate by the average number of liners.

4.2.2 Design parameters

Table 6 summarises the dimensions used in the simulations and the number of liners required to maintain a high separation efficiency.

Table 6: Hydrocyclone dimensions.

Dimension	Value	Unit
Body diameter D_c	75	mm
Inlet diameter $D_i n$	21	mm
Length	375	mm
Liners	[40, 64]	-

The hydrocyclone model requires an oil bubble distribution to calculate the outlet concentration and is summarised in Table 7[28].

Table 7: Parameters for oil droplet distribution used in the hydrocyclone model.

Parameter	Value	Unit
Distribution	Normal distributed	
Standard deviation,	30 σ	μm
Minimum size	1	μm
Maximum size	150	μm

The estimated calculations of the dimensions and the parameters for oil droplet distribution are shown in Appendix B.2.

4.3 Induced gas flotation

The flotation unit was simulated in Matlab and take basis in calculating the number of collisions between oil and gas bubbles in the column. The number of collisions per unit time is also multiplied by the capture efficiency, E, which describes how many of the collision results in capture. The model is presented in Appendix A.3.

4.3.1 Model assumptions

The following assumptions were made to simulate the induced gas flotation.

- The efficiency of oil removal is governed by the probability of collision in the tank.
- Uniformly distributed gas and oil droplets in the tank.
- One dimensional and laminar flow in the tank.
- The rise velocity of the gas bubbles follows Stokes' law.
- The oil droplet velocity is equal to the bulk flow velocity in the tank.
- Oil drops can not detach from gas bubbles once its captured.
- Constant gas and oil droplet radius, r_g and r_o.
- The oil droplet radius can be calculated as the average of the outlet distribution from the hydrocyclone.
- Constant capture efficiency, E.
- The tank has no internal configuration, that is, it is modelled as a simple tank.
- Counter current gas and liquid flow.

4.3.2 Design parameters

Table 8 summarises the gas specifications used in the simulation.

Table 8: Gas specifications used in the IGF model.

Parameter	Value	Unit
Gas radius	400	μm
Gas density	1.205	$\frac{kg}{m^3}$
Gas flow Case 1	0.0033	$\frac{m3}{s}$
Gas flow Case 2	0.02	$\frac{m3}{s}$
Capture efficiency, E	$\frac{1}{1000}$	-

Table 9 summarises the dimensions of the flotation tank used in the simulation.

Table 9: Induced gas flotation dimensions.

Dimension	Value	Unit
Height	2	m
Radius tank	0.5	m
Volume tank	1.5708	m^3

All the presented dimensions and specifications are calculated and discussed in Appendix B.3.

5 Process Description

An overall simplified picture of the whole subsea process is shown in Figure 4. Oil, gas, water and sand are pumped from the well and into the separation system. The well stream is separated into four outlet streams in the separator. Sand, including sludge and other solids, is taken to subsea sand storage after sand handling. Further, the water outflow is separated and then discharged into the seawater when the disposal requirements are achieved. After treating the oil, it is sent for boosting. The gas outflow is sent to gas treatment, followed by gas compression and cooling. After handling the oil stream and gas stream they are gathered in a pipeline and finally transported to the floating production, storage and offloading (FPSO), which is placed 150 km from the production reservoair.

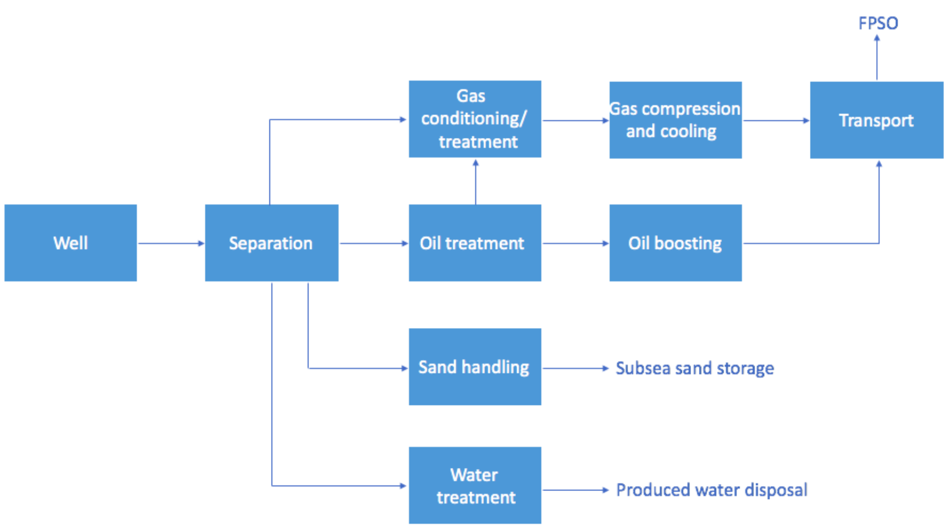

Figure 4: Overall schematic flow sheet of subsea processing system.

The objective of the subsea separation and water treatment is to be able to discharge the water directly into the seawater. To be able to do this, the oil content in the waste water must then be less than 30 ppm [6]. There are several possible designs to reach this requirement, but the main question is, however, how to make the process efficient and economic yet achievable. Three different cases have been modelled to reach the disposal regulations. The first separation step in every case is separation of the well stream by a three-phase gravity separator. Due to a large volumetric inflow, the dimensions of having one separator became very large, which is not practical in terms of installation subsea[62]. Therefore, it was decided to design two smaller separators in parallel by splitting the inflow. Sand, wax and asphaltenes, from the production reservoir, is out of this project' scope, and is therefore neglected. The same applies for oil and gas treatment, and operations which occur after the flow enters the FPSO.

5.1 Case 1

In case 1, the well stream is first separated in two three-phase gravity separators, in parallel, to perform the main separation of gas, oil and water. The water outflow is then separated in one hydrocyclone, followed by one flotation unit. The flotation unit utilises the produced natural gas. The flow sheet of this process design is shown in Figure 5.

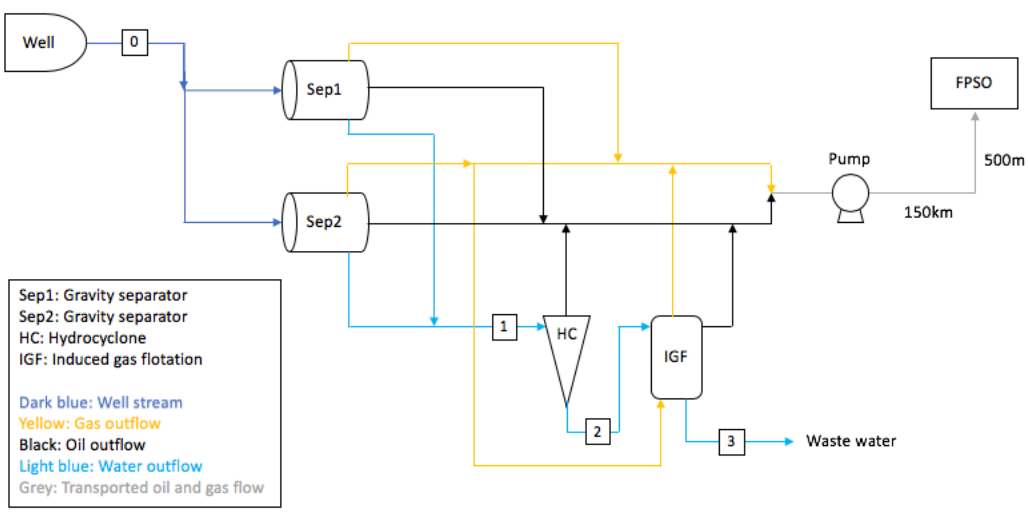

Figure 5: Flow sheet of the design in case 1.

5.2 Case 2

In case 2, the well stream is first separated in two three-phase gravity separators, in parallel, to perform the main separation of gas, oil and water. After the gravity separators, the water outflow is sent to two hydrocyclones designed in series. The flow sheet of this process design is shown in Figure 6.

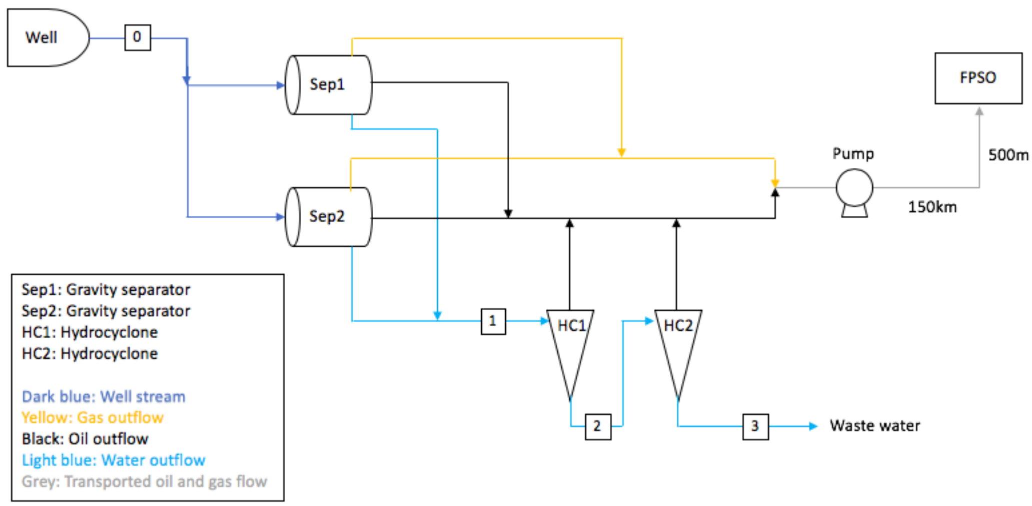

Figure 6: Flow sheet of the design in case 2.

5.3 Case 3

In case 3, the well stream is first separated in two three-phase gravity separators, in parallel, to perform the main separation of gas, oil and water. Then, the water outflow is sent to two flotation tanks designed in series. Both the flotation utilises the natural gas. The flow sheet of this process design is shown in Figure 7.

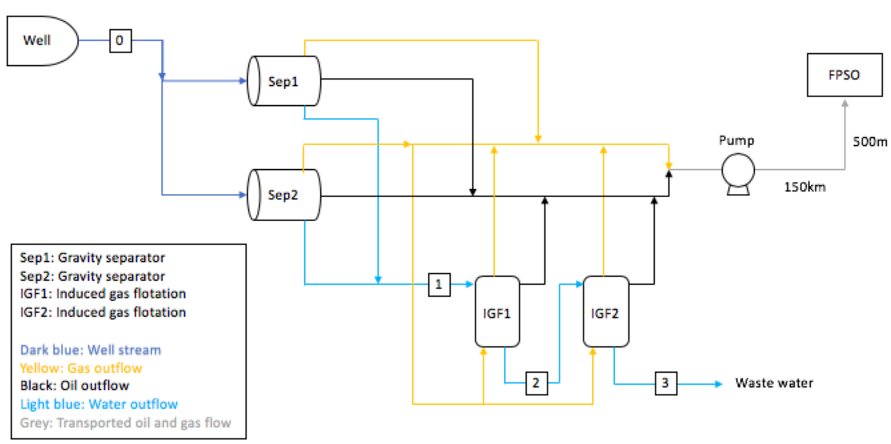

Figure 7: Flow sheet of the design in case 3.

6 Flow sheet Calculations

The designs of the three cases are based on the subsea separation of oil, gas and water. The separation is modelled in Matlab and is presented in Appendix A. The following assumptions were made for all three cases when simulating the separation processes,

- Oil and gas treatment are not included.
- Sand handling system is neglected.
- Wax, ashpaltenes and other problems associated to flow assurance are not considered.
- All operations after FPSO is neglected.
- For year one the water production is zero and therefore not presented in the results.

6.1 Case 1

The flow sheet for the water treatment in case 1 is shown in Figure 8.

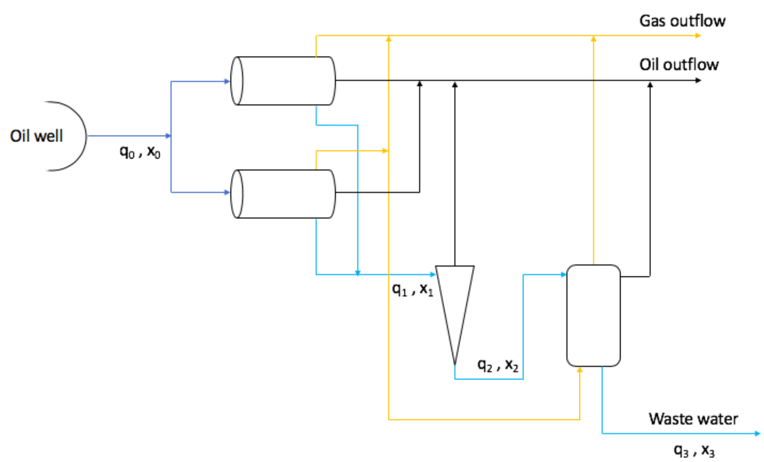

Figure 8: Flow sheet of the subsea separation and water treatment in case 1, with two gravity separators, one hydrocyclone and one flotation unit. The dark blue line represents the well stream, the yellow line represents the gas outflow, the black line represents the oil outflow and the light blue line represents the water outflow.

Table 10 shows the oil mass fractions for the inlet x_0, gravity outlet separator, x_1, outlet hydrocyclone vessel, x_2, outlet flotation unit, x_3, fractions. Given the design parameters presented, the system reaches a maximum outlet concentration of 23.7ppm which is below the required value of 30ppm.

Table 10: Key results from case 1.

Production profile	x_0	x_1	x_2	x_3
Maximum oil production	0.8861	0.3913	0.0516	0.0237
Minimum oil production	0.0449	0.0218	0.0015	0.0014
Maximum liquid production	0.4630	0.2546	0.0187	0.0169

Figure 9 gives a graphical representation of the evolution of the outlet oil fraction from the different units. The blue dots represents the oil fraction out of the reservoir, the orange dots represents the oil fraction out of the gravity separators, the yellow dots represents the oil fraction out of the hydrocyclone and the purple dots represents the oil fraction out of the flotation unit. The y-axis shows the oil fraction in the water outflow, and the x-axis gives the time in years. The exact values for the volumetric flows and it's corresponding mass fractions are given in Appendix C.1.

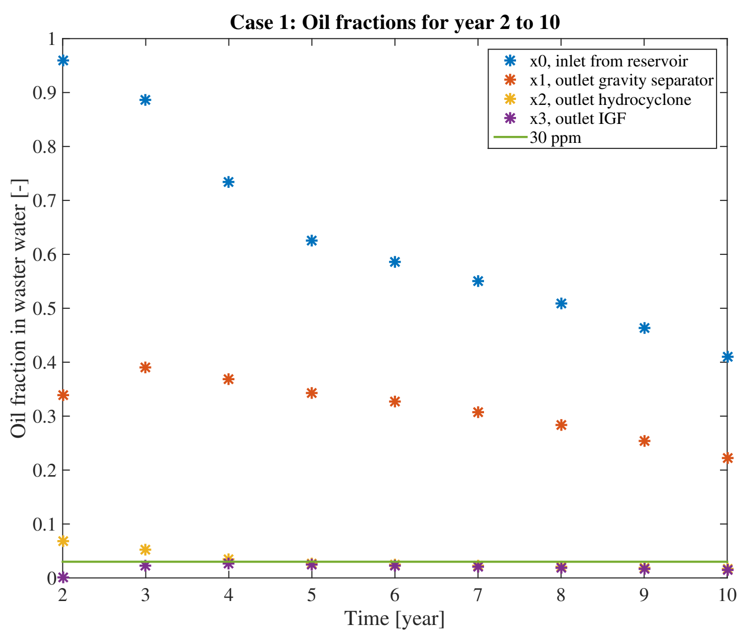

Figure 9: Graphical representation of the of the oil-in-water content for year 2-10 for case 1.

Figure 10 shows how the liquid flows change during years 2 to 10. The blue dots represents the inlet flow from the reservoir. The orange, yellow and purple dots represents the outlet liquid flows from the gravity separator, hydrocyclone and flotation unit, respectively.

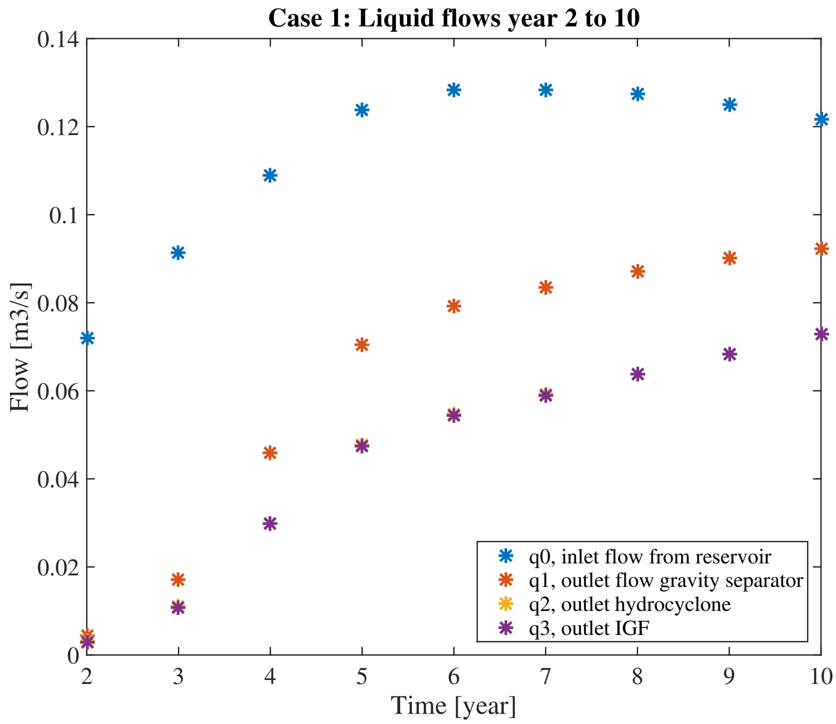

Figure 10: Graphical representation of the inlet liquid flows and outlet liquid flows for the gravity separator, hydrocyclone and IGF for case 1.

As seen in Figure 9, the efficiency of the gravity separators changes during the years. This is due to the variation of the inlet liquid flow. For year two the liquid production is low, thus resulting in a larger residence time and a larger separation efficiency. During the plants lifetime the liquid flow increases, which gives less residence time. At the same time, the inlet oil fraction will also decrease resulting in an overall decreasing outlet oil fraction.

The hydrocyclone yields the largest outlet oil fraction during the years with the lowest liquid production. Since the hydrocyclone is dependent of the tangential force created at the inlet, and smaller velocities create less drive, the years with lowest liquid production will result in the lowest efficiency.

6.2 Case 2

The flow sheet for the water treatment process in case 2 is shown in Figure 11.

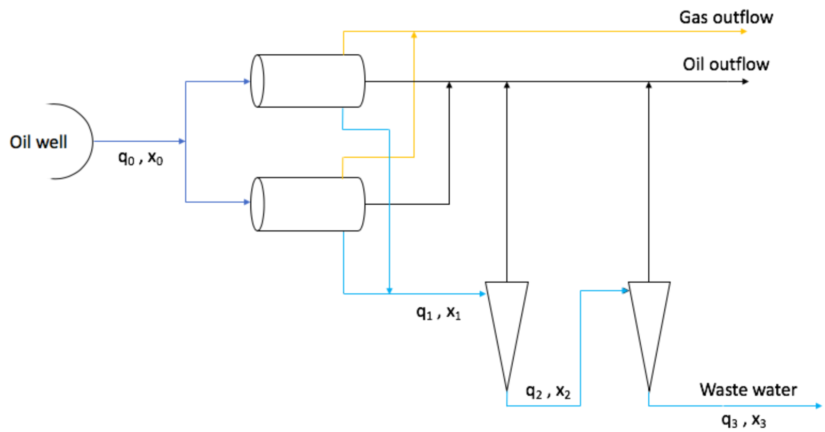

Figure 11: Flow sheet of the subsea separation and water treatment in case 2, with two gravity separators and two hydrocyclones. The dark blue line represents the well stream, the yellow line represents the gas outflow, the black line represents the oil outflow and the light blue line represents the water outflow.

Table 11 shows the oil mass fractions for the inlet x_0, outlet gravity separator, x_1, outlet of first hydrocyclone vessel, x_2, and the outlet of second hydrocyclone vessel,x_3, fractions. Given the design parameters presented, the system reaches a maximum outlet concentration of 6.5ppm which is below the required value of 30ppm.

Table 11: Key results from case 2.

Production profile	x_0	x_1	x_2	x_3
Maximum oil production	0.8861	0.5888	0.0537	0.0065
Minimum oil production	0.0449	0.0313	0.0016	0.000134
Maximum liquid production	0.4630	0.3433	0.0180	0.0150

Figure 12 gives a graphical representation of the evolution of the outlet oil fraction from the different units. The blue dots represents the oil fraction out of the reservoir, the orange dots represents the oil fraction out of the gravity separators and the yellow and purple dots represents the oil fraction out of the first and second hydrocyclone, respectively. The y-axis shows the oil-in-water fraction, and the x-axis gives the time in years. The exact values for the volumetric flows and its corresponding mass fractions are given in Appendix C.2.

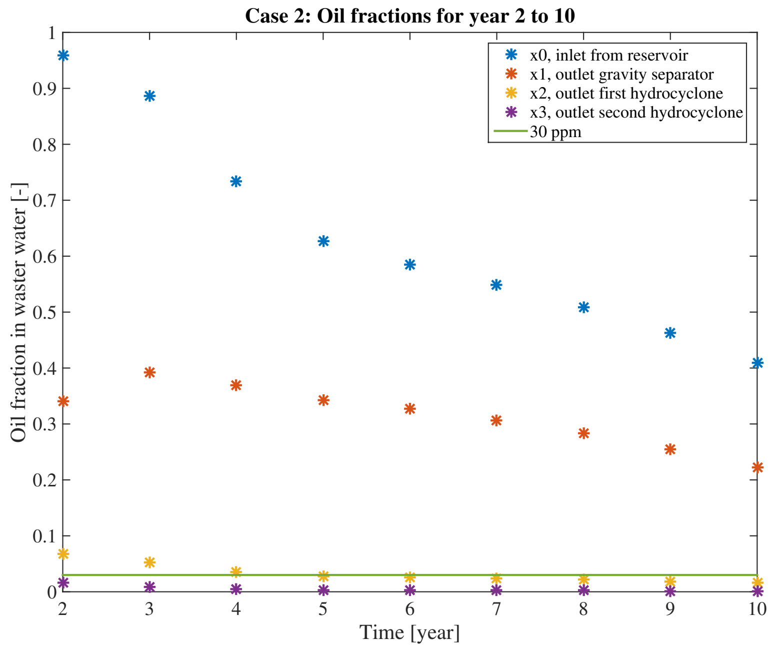

Figure 12: Graphical representation of the of the oil-in-water content for year 2-10 for case 2.

Figure 13 shows how the liquid flows change during years 2 to 10. The blue dots represents the inlet flow from the reservoir. The orange, yellow and purple dots represents the outlet liquid flows from the gravity separator as well as the first and second hydrocyclone, respectively.

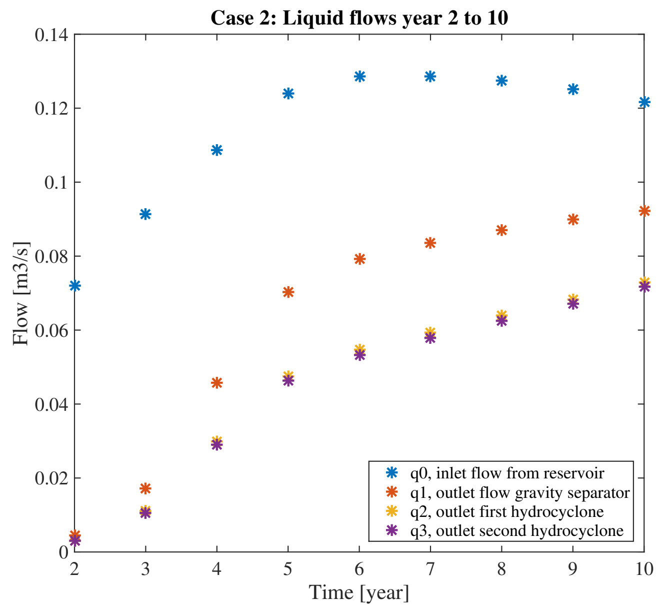

Figure 13: Graphical representation of the inlet liquid flow and outlet liquid flows for the gravity separator, first and second hydrocyclone in case 2.

6.3 Case 3

The flow sheet for the water treatment process in case 3 is shown in Figure 14.

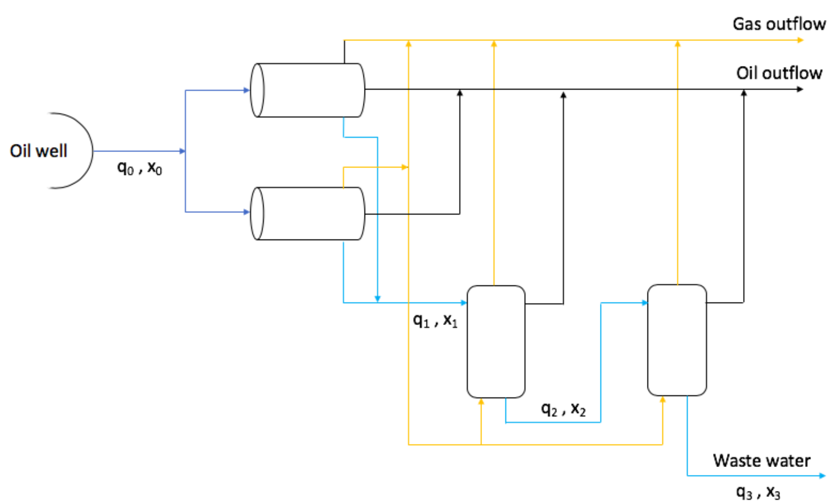

Figure 14: Flow sheet of the subsea separation and water treatment in case 3, with two gravity separators and two flotation units. The dark blue line represents the well stream, the yellow line represents the gas outflow, the black line represents the oil outflow and the light blue line represents the water outflow.

Table 12 shows the oil mass fractions for the inlet x_0, outlet gravity separator, x_1, outlet of first flotation tank, x_2 and outlet of second flotation, x_3, fractions. Given the design parameters presented, the system reaches a maximum outlet concentration of 30ppm, which just at the boarder of the required value of 30ppm.

Table 12: Key results from case 3.

Production profile	x_0	x_1	x_2	x_3
Maximum oil production	0.8861	0.3913	0.0005	≈ 0
Minimum oil production	0.0449	0.0218	0.0098	0.0044
Maximum liquid production	0.4630	0.2546	0.1003	0.0300

Figure 15 gives a graphical representation of the evolution of the outlet oil fraction from the different units. The blue dots represents the oil fraction out of the reservoir, the orange dots represents the oil fraction out of the gravity separators, the yellow dots represents the oil fraction out of the first flotation unit and the purple dots represents the oil fraction out of the second flotation unit. The y-axis shows the oil fraction in the water outflow, and the x-axis gives the time in years. The exact values for the volumetric flows and it's corresponding mass fractions is given in Appendix C.3.

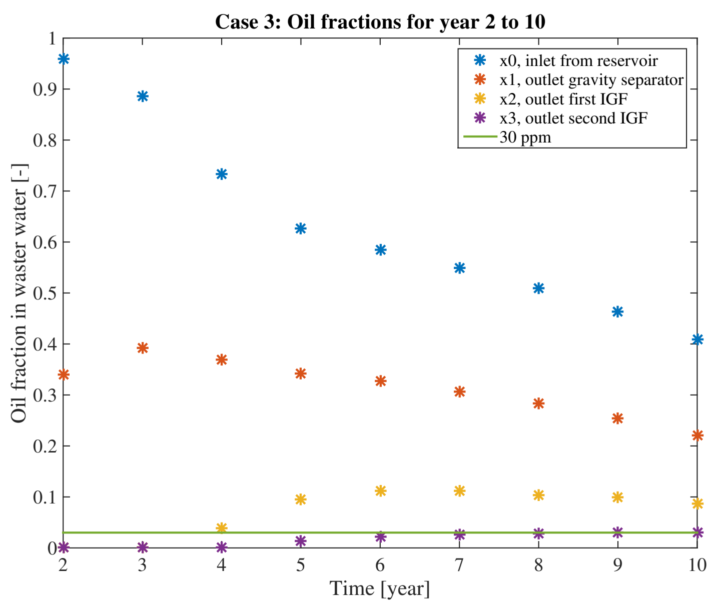

Figure 15: Graphical representation of the of the oil-in-water content for year 2-10 for case 2.

Figure 16 shows how the liquid flows change during years 2 to 10. The blue dots represents the inlet flow from the reservoir. The orange, yellow and purple dots represents the outlet liquid flows from the gravity separator as well as the first and second hydrocyclone, respectively.

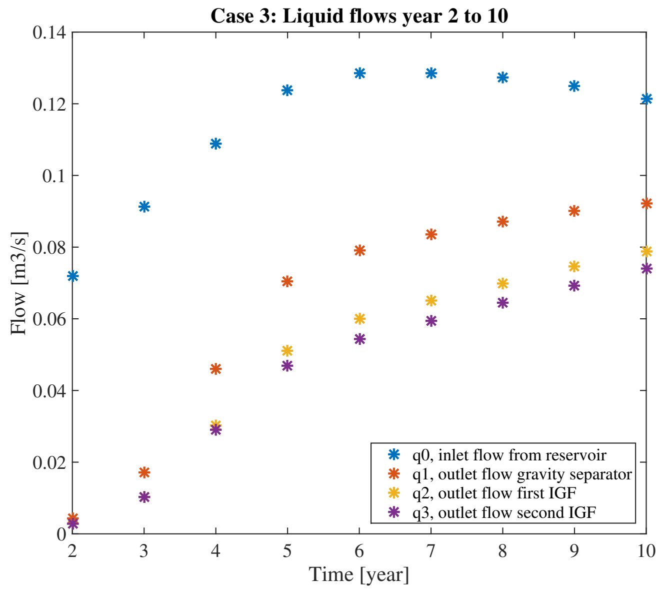

Figure 16: Graphical representation of the inlet liquid flow and outlet liquid flows for the gravity separator, first and second IGF.

As seen in Figure 15, the flotation units will be most effective during the years with the lowest liquid production. When the flow is small, the velocity inside the tank will decrease which gives an increased residence time. An increased residence time will result in more oil-bubble collisions and therefore improve the separation efficiency.

7 Case discussion

Due to sparse sources on subsea water treatment, the discussion is based on available information and simulations. Practical issues regarding installation and testing is not taken into consideration, and the estimated cost could therefore be larger than the values presented below.

7.1 Cost

Cost comparison of the three cases are based on the total investment cost. Neither the gravity separator, hydrocyclone or flotation unit requires a significant amount of power, and it is therefore neglected when comparing the different cases. The other fixed equipment like the oil and refining, piping, valves and sand handling systems are also left out of the cost comparison. The three cases also requires different umbilical lengths and piping systems, but it is left out of the estimation. The installation cost for single units as well as the total investment for equipment are shown in Table 13, 14 and 15.

Table 13: Cost estimation for the components used in case 1.

Component	Installation cost [USD]
Gravity separator $\times$ 2	7 183 888
Hydrocyclone	803 981
Flotation unit	2 381 208
Sum	**10 369 077**

Table 14: Cost estimation for the components used in case 2.

Component	Installation cost [USD]
Gravity separator $\times$2	7 183 888
Hydrocyclone	803 981
Hydrocyclone	803 981
Sum	**8 791 850**

Table 15: Cost estimation for the components used in case 3.

Component	Installation cost [USD]
Gravity separator $\times$2	7 183 888
Flotation unit	2 381 208
Flotation unit	2 381 208
Sum	**11 946 304**

Comparing the cost estimations and total equipment costs, case 2 with two hydrocyclones in series yields the lowest total equipment cost. Case 3 was, on the other hand, the most expensive alternative. Flotation devices are often more expensive compared to hydrocyclones due a more complex inner structure and size[20]. Looking exclusively at the cost, case 2 is the obvious choice.

7.2 Operation

To minimize the need for maintenance a subsea plant should be simple and robust[14]. The water treatment system also needs to be reliable and able to handle the changing flow rates and composition during the plants lifespan. These are the two main criteria when evaluating the cases.

Comparing the operation performance, case 2 yields the overall lowest outlet concentration. In addition, given that the flow in each liner does not exceed a certain maximum value, hydrocyclones operates with the same efficiency independent of the inlet oil concentration and liquid flow, which gives a steady and predictable efficiency during the whole lifespan of the plant. Even though wax and sand handling are out of the scope for this project, a practical problem with hydrocyclones are blockage. The blockage can therefore affect both of the units making the system less robust. This would also contribute with a higher maintenance and inspection cost. Regular back flushing and automatic cleansing are therefore required which could result in less operating time[17]. In addition, hydrocyclones are only effective for a certain size range of oil droplets. To what degree the model describes the bubble distribution is questionable, and a deviation from the real distribution could cause the final concentration to be much larger than the model predicts. Taking all factors into consideration, case 2 represents an efficient and low cost alternative.

The counterpole of case 2 is case 3, with two flotation units in series it represent the most expensive and least effective alternative. Flotation units are also more affected by the liquid flow rates compared to hydrocyclones, making the water treatment system more vulnerable during the years with large liquid production. A possible solution is to increase the dimensions, but since the process will be located subsea this can be inconvenient. However, the efficiency can also be controlled by increasing the gas stream, thus making the units more adaptable for coping changing flow rates. Flotation units also allows for the possibility of recycling. Even though this will increase the flow velocity inside the unit, thus resulting in a lower residence time, obtaining an acceptable oil removal can be compensated by increasing the gas stream. Therefore, case 3 also represent a possible alternative, but is rejected because of the relatively large cost and overall poor efficiency.

Case 1 represents the middle path between case 2 and 3, both in terms of investment cost and outlet oil concentration. By placing them in series, with the hydrocyclone taking care of the main separation and the flotation unit removing the remaining oil of all sizes, makes the system able to cope with both different flows and variable oil droplet distributions.

7.3 Case conclusion

All the cases have their advantages and disadvantages. Case 2 represents the most economical solution, but could provide problems if the real oil droplet distribution deviates from what the model assumes. Being precautionary, a flotation unit could be necessary to ensure the most reliable water treatment system. All taken into consideration, even though the investment cost is larger for case 1, the advantages outweighs the price difference. Case 1 was therefore chosen to be the best alternative for this plant.

8 Cost Estimation

Subsea cost is a term that describes the whole project, from the strategy selection to the abandonment of the project. For a subsea field development, both the capital expenditures(CAPEX) and the operation expenditures(OPEX) are a part of the cost. For a typical project, the CAPEX is usually the 2 to 3 first years of the project, and it includes strategy selection, bids, exploration and operation, feasibility studies and project execution. The OPEX, typical the next 5 to 50 years, includes production and maintenance, and abandonment of the project. A full cost estimation was only performed for Case 1, which will be presented in this chapter.

8.1 Capital Expenditures(CAPEX)

The CAPEX of this project includes the necessary equipment to perform subsea separation. This includes gravity separators, a hydrocyclone and an induced gas flotation unit for the water treatment. Also, it includes flowlines and riseres, umbilicals included electrical power cables, subsea hardware, control equipment, testing cost and engineering, insurance and contingency[14]. In addition to this, drilling, subsea trees and manifolds are a big part of the regular CAPEX cost for a subsea system. In this case, an already existing oil field with necessary infrastructure is assumed to be available. Therefore, these costs are neglected in this project, as they are already installed. For the sand handling, this is out of this projects scope and neglected.

The CAPEX costs is calculated using different methods. The gravity separator is estimated based on size and required shell mass. The IGF unit and hydrocyclone are based on historical values. All the estimated costs for the water treatment system are scaled to account for subsea instalment, process control, material, engineering work, insulation and inflation.

The remaining cost were found from a CAPEX example presented in the Subsea Engineering Handbook[14], which summarised the main expenditures regarding subsea oil production systems. These values is based on a previously executed project in the Gulf of Mexico during 2007. The facility was installed at a water depth of 1371 meters. Since the presented example includes the additional expenditures for subsea instalment and splits the equipment, process control, testing and engineering work into different sections, the values were only scaled accordingly to the 2018 Chemical Engineering Plant Cost Index, CEPCI.

8.1.1 Gravity Separator

The gravity separator was cost estimated with the use of correlations from purchased equipment cost for common plant equipment, and then further scaled to installed cost in current time. The correlations used represented a horizontal pressure vessel made of stainless steel. A detailed calculation of the cost estimation can be seen in Appendix D.5. The final cost of the gravity separator is shown in Table 16.

Table 16: Cost estimation gravity separator.

Component	Installed cost [USD]
Gravity Separator	3 591 944

8.1.2 Hydrocyclone

The cost estimation for the hydrocyclone take basis in historic cost data. Estimating based on the inlet flow resulted in an installed cost of 367 880 USD. Due to the relative low cost compared to the other units, the estimation was also compared to different historical costs. A beef processing facility published purchase and instalment costs of a similar hydrocyclone used in deoiling which yielded a final cost of 500 194 USD. The cost was also estimated based on body diameter and number of liners which is presented in Table 44, and was chosen for further calculations. A detailed calculation of the cost estimation can be seen in Appendix D.6.

Table 17: Cost estimation hydrocyclone.

Component	Installation cost [USD]
Hydrocyclone	803 981

8.1.3 Induced Gas Flotation unit

The cost estimation for the flotation unit take basis in historic cost data[32]. The data was given for a dissolved gas flotation unit, which is a similar process to induced gas flotation[34]. Dissolved gas flotation units often requires a higher capital cost, and the final cost could therefore be an overestimation[40]. The reference cost includes all necessary tankage, pumps, motors, and control instrumentation, and is shown in Table 46. A detailed calculation of the cost estimation can be seen in Appendix D.7.

Table 18: Cost estimation for the induced gas flotation unit.

Component	Installation cost [USD]
Induced gas flotation	2 381 208

8.1.4 Flowline and riser

The pipeline transporting both oil and gas to the FPSO, is set to be 12inches (0.3048m) for the whole design. The flowline is assumed to be rigid, while the riser is assumed to be flexible. The final installed cost is shown in Table 19. A detailed calculation of the cost estimation can be seen in Appendix D.8.

Table 19: Cost estimation for flowline and riser.

Component	Installed cost
Flowlines and riser	135 348 043

8.1.5 Umbilicals

The cost of the umbilical includes electrical power cable, signal cable and conduit for hydraulic control fluid. The final installed cost is shown in Table 20. A detailed calculation of the cost estimation can be seen in Appendix D.9.

Table 20: Cost estimation umbilical.

Component	Installed cost [USD]
Umbilical	258 022 426

8.1.6 Subsea Hardware

Subsea hardware is necessary for instalment of the separator and water treatment units and is therefore included in CAPEX. Suction piles used as a foundation for pipelines initiations and terminations and effective anchors[43]. Pipeline End Termination (PLET) are used in new constructions where the pipeline terminates or needs to be jumpered to a different location like a tank or a refinery[44]. Pigging is required to to recover residual liquid in pipelines[45]. Flying Leads are used to link subsea structures such as manifolds, trees and umbilicals[46]. A multiphase flowmeter is a device used to measure the flow of different phases before the separation of oil, water and gas[47]. The estimated costs excludes testing and control equipment. The cost for the individual components and the total cost estimation are shown in Table 21.

Table 21: Hardware cost.

Hardware type	Installed cost USD]
Suction Pile	1 125 485
Production PLET	3 903 597
Production Tree Jumpers	1 097 544
Pigging	485 708
Production PLET Jumpers	2 022 353
Multiphase Flow Meter	1 040 229
Flying Leads	1 403 515
Sum	**11 078 413**

8.1.7 Control equipment

The topside control equipment includes a hydraulic power unit, master control station, umbilical termination assembly(SUTA), and an electrical power unit[14]. The required units and the final instalment cost is presented in Table 22.

Table 22: Control equipment installed cost.

Control type	Installed cost [USD]
Topside control	3 340 107
Tree-Mounted control	5 750 037
SUTA	3 111 764
Sum	**12 201 908**

8.1.8 Testing cost

Testing necessary equipment before production starts is a crucial before production start. The values were obtained using historical cost data[14]. Table 52 presents the main testing costs for hardware and commissioning. The values refer to either Factory Acceptance Testing(FAT), Site Integration Testing(SIT) or Extended Factory Acceptance Test (EFAT). Where SIT is testing to verifying the whole system works together independently of the suppliers. FAT and EFAT includes testing of subsea installation equipment before instalment to check for required efficiency and function. To what extent the testing cost gives a correct estimation is questionable. Building a project upon new technology will contribute with a much larger testing cost. Taken into consideration that subsea water treatment is relatively unexplored area, the final testing cost could possible be much higher than the values estimated in Table

23.

Table 23: Testing cost.

Type	Final cost [USD]
Subsea Hardware FAT, EFAT	30 536 850
Tree SIT and Commissioning	984 799
PLET SIT	636 460
Control System SIT	267 624
Sum	**32 425 733**

8.1.9 Engineering, insurance and contingency

Based on historical cost data, the engineering work, insurance and contingency cost was estimated[14]. The engineering work will be dependent on the technology development and a well tested subsea facility based upon tested technology will require less engineering hours. Since there are generally little subsea water treatment experience to build upon, the total engineering cost could therefore be much higher than presented[7]. Table 24 summarises the estimations.

Table 24: Engineering, insurance and contingency costs.

Type	Final cost [USD]
Engineering and Project Management Cost	5 333 030
Insurance	6 755 172
Contingency and Allowance	14 135 577
Sum	**26 223 779**

8.1.10 Total installation cost

The total CAPEX was obtained by summarising all the individual costs and is shown in Table 25.

Table 25: Total installation equipment cost.

Type	Cost[USD]
Gravity separators	7 183 888
Hydrocyclone	803 981
Flotation Unit	2 381 208
Flowline and Riser	135 348 043
Umbilicals	258 022 426
Subsea Hardware	11 078 413
Control equipment	12 201 908
Testing Cost	32 425 733
Engineering, Insurance and Contingency	26 223 779
Total Cost	**485 669 379**

8.2 Operating expenditures (OPEX)

The operating costs are the costs of producing the product. It is necessary with an estimate of this cost to evaluate the viability of the project, and to choose between different processing schemes. The operating costs are divided into two types of costs: the fixed operating costs and the variable operating costs. The fixed operating costs do not vary with the production rate, and the variable operating costs is varying with the amount of produced product. The fixed costs include among others maintenance, operating labour, laboratory costs, supervision and insurance. The variable operating costs contains raw materials, miscellaneous operating materials, utilities and shipping and packaging[15]. The variable chemicals is approximately 2% of the OPEX[14] and is neglected. The main operating costs are maintenance and power cost, and are therefore the only costs considered as operating costs in this case.

The maintenance cost for a plant consists of the cost of maintenance labour and material used for maintenance of the process. For chemical plants, this is the main annual cost. The maintenance is usually estimated to be between 3% to 5% of the ISBL investment for onshore plants. This value vary with the plants reliability, and the amount of solids handling or moving equipment[16]. For this subsea process, it is assumed that the maintenance cost is 5% of the total CAPEX.

A previous thesis written about subsea separation, investigating boosting and fluid transport with a similar design, concluded with an annual power cost of 3 149 856 USD for year 1-6 and 2 725 142 USD for later production[61]. Using an average will provide sufficient information considering power cost is out of this projects scope. This was calculated by the assumption that the plant operates 8000 hours per year [61]. The total annual OPEX cost is shown in Table 26.

Table 26: Total annual operating expenditures(OPEX) for unit costs and total cost.

Type	Cost [USD]
Power	2 937 499
Maintenance	24 283 469
Total annual OPEX	**27 220 968**

9 Investment Analysis

An investment analysis was performed to investigate the projects profitability. The assumptions for the analysis is presented below.

- The plant has an economical lifetime of 10 years.
- The present value of the equipment after 10 years is zero.
- The discount rate equals 10% in the NPV calculations[50].
- The marginal tax rate is 78%[51].
- The cashflow is only determined by the oil and gas production.
- No loans are raised, which means that the equity covers 100% of the total investment.
- 8000 working hours a year.
- Zero working capital, due to low labour costs.
- Depreciation is neglected.

9.1 Profitability of the project

The profitability of the project depends on sales revenue, CAPEX and OPEX. There are four main measures to evaluate the profitability: Net Present Value(NPV), Return on Investment(ROI), Internal Rate of Return(IRR) and the pay-back time(t_{pb}). These indicators were calculated using the detailed procedure shown in Appendix D, and are given in Table 27.

Table 27: Profitability measures: Net present value, return on investment, internal rate of return and payback time.

Profitability measures	Value	Unit
NPV	658.27	mill. USD
ROI	38.07	%
IRR	37.67	%
t_{pb}	3.12	years

To visualise the profitability of the project, a cash flow diagram was plotted, as shown i Figure 17. The cash flow accounts for the total investment, operating costs, income and taxes.

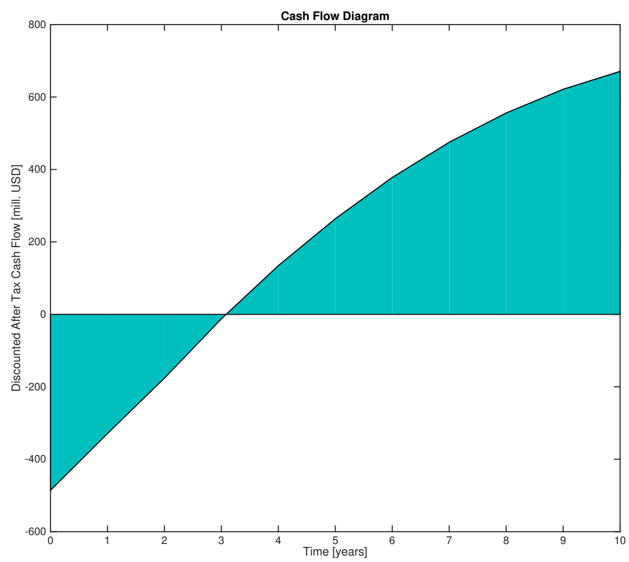

Figure 17: Cash flow diagram when CAPEX, OPEX, taxes and net income is the only factors that is taken into account.

Year zero accounts for the total investment cost, and the following years accounts for the net cash flow in each year. The shaded area below the intersection of the x-axis represents the payback of the total investment. The crossing point of the x-axis is therefore equivalent to the pay-back time, here approximately 3 years. When the cash flow is positive the shaded area represents the total profit.

9.2 Sensitivity analysis of the investment

The sensitivity analysis investigates how the viability of the project changes with uncertainties in different parameters. The analysis takes basis in how the total NPV changes if the CAPEX, OPEX or oil price varies in the range of ± 60% and is presented in Figure 18.

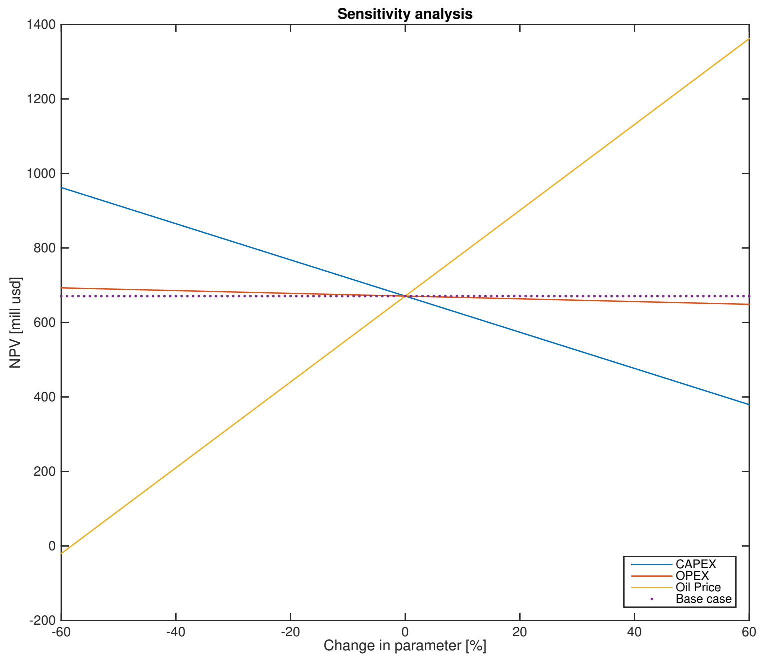

Figure 18: Sensitivity analysis. CAPEX, OPEX and the oil price varies in the range of ± 60%.

The steeper curve, the higher degree of sensitivity. From the sensitivity analysis it can be seen that a deviation in the oil price has the largest impact on the total net present value. The break-even oil price was found, from reading directly of the graph, to be approximately 28.14 USD/bbl.

10 Discussion

The goal of the subsea separation and water treatment system was to make an adaptable and robust system able to cope with changing inflow and composition. Case 1 had all these capabilities. According to the simulation results, the oil-in-water fraction achieved the disposal requirement. The system also benefited from the fact that the hydrocyclone operated with the greatest efficiency during the years of large liquid production, while the efficiency of the IGF unit peaked during the years with lowest liquid production. The system was also capable of treating all ranges of oil emulsions and took into account that the distribution used in simulations could be inaccurate.

There are also uncertainties linked to the model results. Since the efficiency of the gravity separator is user specified, the actual separation will deviate from the model results. The constant was, however, chosen pessimistically. After consideration and guidance, the constant was lowered to yield a lower efficiency to rather underestimate the performance. There were multiple sources claiming a 90% efficiency for the hydrocyclone under certain liquid flows [17][31][33], which are consistent with the results. The main source of error is, however, the oil droplet distribution. A distribution shifted towards the left, that is, the emulsion generally consists of smaller oil droplets, will result in an overall poorer oil removal.

Since the model describing the gas flotation was based on physical descriptions, the results are uncertain. The large liquid flow will produce turbulence inside the tank which inhibits the possibility for oil and gas bubbles to interact and collide[20]. This is inconsistent with the assumption of laminar flow and could result in an overestimated performance. In addition, it was assumed that the tank had no internal configuration. In practice, IGF units typically have protruding walls, making the overall path larger to increase the residence time and efficiency[20]. The possibility for detachment of oil from gas bubbles, once captured, is also neglected and will accordingly overestimate the overall efficiency. However, when examining the performance for case 3, both units operated with a removal efficiency of 50% which is consistent with experimental values under similar conditions[59]. It is hard to determine if the compliance is random, but indicates that the model could give a reasonable estimate of the performance under certain conditions.

Besides making a robust separation and water treatment system, the project also has to be financially viable. According to the profitability analysis, a subsea facility with fully integrated separation and water treatment system still gave a large net present value, return of investment and a low payback time. There are, however, major uncertainties linked to the estimates. Since subsea separation and water treatment is a relatively unexplored field, the testing and engineering costs could potentially be much higher than estimated. In addition, the operating costs could deviate in case of unpredicted events linked to the separation system. Untested technology usually requires several improvements before the reliability is acceptable. New technology do also, in general, contribute with a larger longevity uncertainty.

Considering the total cost, the project is profitable. In what degree the estimated cost gives a realistic picture of the total cost is however questionable. The major cost estimations were obtained from a subsea project based on a different geographic location with a water depth of 1371 meters. Sea depth is usually one of the largest cost driving factors, and could contribute to a higher CAPEX than predicted[14]. There are, however, several reasons to believe that the total cost is underestimated instead of overestimated due to engineering and testing costs. Choosing a fixed 5% of maintenance is also both an oversimplified and inaccurate estimate. However, as presented in the sensitivity analysis, the OPEX does not have a large impact on the total profitability. The most critical factor when considering the profitability is the oil cost. During the last years, the oil price has been a roller coaster of fluctuations[8]. From the sensitivity analysis, a 58% decrease in oil price, that is, an oil price of 28.14 $\frac{USD}{bbl}$, will result in a negative net present value, given that OPEX and CAPEX remain constant. At the 17th of January 2016, the oil price dropped to an all time low of 28.91$\frac{USD}{bbl}$[41]. Therefore, even tough the oil price has shown an increasing trend during the last years, investing in the petroleum industry will be linked to major uncertainties[41].

11 Conclusions and Recommendations

A subsea separation and water treatment system is a possible solution in the future. Since physical maintenance and inspections are limited subsea, adopting existing and proven technology can contribute with a more predictable system. By making smart design the process can achieve the disposal criteria for all liquid flows and compositions. A subsea separation and water treatment system could also contribute with a profitably and robust solution. Case 1 fulfilled all these requirements. However, the lack of available subsea water treatment information makes it difficult to decide which case would work in practice.

As of now, when the technology is still in research phase, it is difficult to make a decision whether a fully integrated subsea separation and water treatment system is viable and profitable. The area does, however, have a lot potential. Given that other technology challenges, like a reliable measurement device to constantly monitor the oil-in-water content, gets solved, subsea water treatment systems could in the future provide cheaper and more efficient solutions.

List of Symbols

Table 28: List of Symbols.

Symbol	Description	Unit
a	Cost constant	-
A_c^v	Vapour cross-sectional area	m^2
A_c^l	Liquid cross-sectional area	m^2
b	Cost constant	-
c_3, c_4, c_5	Empirical constant	-
$CAPEX_i$	Capital expenditures of period i	USD
CF	Net annual cash flow	USD
CF_a	Average cash flow	USD
C_0	Historical cost	USD
C_1	Historical installation cost	USD
C_2	Installation cost in 2018	USD
C_{misc}	Miscellaneous cost	USD
d	Drop diameter	m
d_{75}	Droplet diameter when 75% of the drops are separated	m
$\tilde{d_{75}}$	Reduced drop diameter	m
D	Diameter	m
D_c	Body diameter	m
D_v	Vessel diameter	m
D_{in}	Inlet diameter	m
E	Capture efficiency	-
f_c	Civil engineering work installation factor	-
f_{el}	Electrical work installation factor	-
f_{er}	Equipment erection installation factor	-
f_i	Instrumentation and process control installation factor	-
f_{inst}	Installation factor	-
f_m	Material installation factor	-
f_l	Lagging, insulation or pain installation factor	-
f_p	Piping installation factor	-
f_s	Structures and buildings installation factor	-
f_{size}	Size factor	-
f_{sub}	Subsea installation factor	-

f_t	flow line type factor	-
f_v	Factor: cross-sectional area occupied by vapour	-
F	Lang factor	-
g	Gravity constant	$\frac{m}{s^2}$
h	Water depth	m
H	Height of tank	m
h_v	Liquid vessel height	m
I	Investment	USD
I_i	CEPCI index for year i	-
$I_{refereance}$	CEPCI index for reference year	-
k	Separator performance constant	-
IRR	Internal Rate of Return	-
L	Length	m
L_v	Vessel length	m
M_p	Migration probability	-
NPV	Net Present Value	-
N_{Hy}	Hydrocyclone number	-
NI_i	Net Income for a period i	USD
n	Exponential cost factor	-
N_{RHi}	Inlet Reynolds number	-
$OPEX_i$	Operational expenditures of period i	USD
P	Pressure	bar
P_{ext}	External pressure	MPa
q_b	Bulk volumetric flowrate	$\frac{m^3}{s}$
q_v	Vapour volumetric flowrate	$\frac{m^3}{s}$
q_l	Liquid volumetric flowrate	$\frac{m^3}{s}$
q_i	Volumetric flowrate of component i	$\frac{m^3}{s}$
q_{in}	Volumetric inflow	$\frac{m^3}{s}$
q_o	Oil volumetric flowrate	$\frac{m^3}{s}$
q_w	Water volumeric flowrate	$\frac{m^3}{s}$
R	Radius	m
R_d	Droplet radius	m
ROI	Return On Investment	-
R_i	Revenue of period i	USD
r	Interest rate	-

r_g	Radius of gas bubble	m
r_o	Radius of oil bubble	m
T	Temperature	°C
t	Time	s
t_h	Liquid hold-up time	s
t_{pb}	Pay-back time	year
t_r	Rate of taxation	-
t_w	Wall thickness	s
S	Size parameter	-
u_s	Settling velocity without demister pad	$\frac{m}{s}$
u_t	Settling velocity with demister pad	$\frac{m}{s}$
V_h	Hold-up volume	m^3
V_{col}	Volume of collision cylinder	m^3
V_i	Volume of i	m^3
V_v	Vessel volume	m^3
v_b	Velocity of oil water bulk flow	$\frac{m}{s}$
v_g	Gas velocity	$\frac{m}{s}$
v_o	Oil velocity	$\frac{m}{s}$
v_{rel}	Relative velocity	$\frac{m}{s}$
v_v	Vapour velocity	$\frac{m}{s}$
v_{in}	Inlet velocity	$\frac{m}{s}$
x_i	Mass fraction of component i	-
$y(d)$	Oil droplet distribution function	-
Z_g	Number of collisions per unit time	-
$\rho_{b,o}$	Density of oil bubbles in tank	$\frac{kg}{m^3}$
ρ_{in}	Inlet density	$\frac{kg}{m^3}$
ρ_g	Gas density	$\frac{kg}{m^3}$
ρ_m	Metal density	$\frac{kg}{m^3}$
ρ_l	Liquid density	$\frac{kg}{m^3}$
ρ_o	Oil density	$\frac{kg}{m^3}$
ρ_v	Vapour density	$\frac{kg}{m^3}$
ρ_w	Water density	$\frac{kg}{m^3}$
τ	Residence time	s
τ_{act}	Actual residence time	s
τ_v	Vapour residence time	s

μ	Dynamic viscosity of fluid	Pa $\cdot s$
σ	Standard deviation	-

List of Abbrevations

Table 29: List of Abbrevations.

Acronym	Description
CAPEX	Capital expenditures
CEPCI	Chemical Engineering Plant Cost Index
DAF	Dissolved Air Flotation
EFAT	Extended Factory Acceptance Test
FAT	Factory Acceptance Testing
FEED	Front-End Engineering Design
FPSO	Floating Production, Storage and Offloading
GOR	Gas Oil Ratio
HIPPS	High Integrity Pipeline Protection System
HSE	Health and Safety Executive
IGF	Induced Gas Flotation
IRR	Internal Rate of Return
ISBL	Inside Battery Limits
NSF	Nut Shell Media Filtration
NTP	Normal Temperature and Pressure
OPEX	Operation expenditures
PSV	Pressure Safety Valve
PWRI	Produced Water Injection
PLET	Pipeline End Termination
QA	Quality Assurance
ROI	Return On Investment
SIT	Site Integration Testing
SUTA	Subsea Umbilical Termination Assembly

References

[1] Tore Irgens Kuhnle, DNV GL Strategic research innovation position paper, 2015: All subsea- Creating value from subsea processing, 2015. Accessed: 21.10.18

[2] Esmaeil Jahanshahi. *Challenges in design, operation and control of subsea separation processes*, October, 2013. Accessed: 21.10.18

[3] Birgitte Nordheim Tveter, *Subsea Processing* https://www.uio.no/studier/emner/matnat/math/MEK4450/h15/ppt/l5/uio-22-sep2015-subsea-processing-birgitte--lecture-notes-23.09.pdf, UiO, 22 September, 2015. Accessed: 21.10.18

[4] FMC Technologies, http://www.fmctechnologies.com/en/SeparationSystems/Technologies/HighPerformanceInternals/SandRemoval.aspx#. Accessed: 21.10.18

[5] Sayda, A. & Taylor, J., *Modeling and Control of Three-Phase Gravilty Separators in Oil Production Facilities* https://www.researchgate.net/publication/4265563_Modeling_and_Control_of_Three-Phase_Gravilty_Separators_in_Oil_Production_Facilities, August 2007. Accessed: 21.10.18

[6] eProcess Technologies, http://eprocess-tech.com/products/oil-water-separation/process/. Accessed: 21.10.18

[7] Dr. Ming Yang, *Dealing with produced water subsea*. https://www.epmag.com/dealing-produced-water-subsea-722996, October 2014. Accessed: 23.10.18

[8] Christiane Baumeister and Lutz Kilian, *Forty Years of Oil Price Fluctuations: Why the Price of Oil May Still Surprise Us*, https://pubs.aeaweb.org/doi/pdf/10.1257/jep.30.1.139, Winter 2016. Accessed: 23.10.18

[9] SS Sidhu, *How Subsea Components Of ROV Sustain Tremendous Seawater Pressure?*, https://www.marineinsight.com/offshore/subsea-components-sustain-tremendous-seawater-pressure/, March 10, 2016. Accessed: 23.10.18

[10] NORSOK STANDARD, *Process Design*, http://www.standard.no/pagefiles/1130/p-001r3.pdf, Rev. 3, November, 1997. Accessed: 23.10.18

[11] Society of Petroleum Engineers, *Subsea processing benefits*, https://petrowiki.org/index.php?title=Subsea_processing_benefits&printable=yes , 2. June, 2015. Accessed: 23.10.18

[12] R.Mastouri,S.M. Borghei, F.Nadim, E.Roayaei, *The investigation of induced gas flotation (IGF) performance at elevated temperatures and high total dissolved solids (TDS) produced water*,

https://www.researchgate.net/publication/228504759_THE_INVESTIGATION_OF_INDUCED_GAS_FLOTATION_IGF_PERFORMANCE_AT_ELEVATED_TEMPERATURES_AND_HIGH_TOTAL_DISSOLVED_SOLIDS_TDS, Islamic Azad University , Arak Branch, Arak, Iran, January, 2009. Accessed: 25.10.18

[13] The Editors of Encyclopaedia Britannica, *Stokes's law* , https://www.britannica.com/science/Stokess-law, 2016. Accessed: 25.10.18

[14] Yong Bai, Qiang Bai, *Subsea Engineering Handbook* Gulf Professional Publishing, 2010. Accessed: 25.10.18

[15] R.K. Sinnott *Chemical Engineering Design* Coulson Richardson's Chemical Engineering series, Vol. 6, 4rt edition, Elsevier, Amsterdam, 2005. Accessed: 21.10.18

[16] Sinnott, R. Towler, G., *Chemical Engineering Design*, Coulson Richardson's Chemical Engineering Series, Vol. 6, 5th edition, Elsevier, Amsterdam, 2009.Accessed: 21.10.18

[17] Dr. John Walsh, *Hydrocyclone Webinar*, http://petrowatertech.com/wp-content/uploads/2015/08/Hydrocyclone-Webinar.pdf, 2013. Accessed: 29.10.18

[18] John Ditria Early Challenges, Progress Development: Part 2, https://www.linkedin.com/pulse/produced-water-treatment-deoiling-hydrocyclones-john-ditria-4, 2017. Accessed: 29.10.18

[19] L.R.Castilho, R.A.Medronho, *A simple procedure for design and performance prediction of Bradley and Rietema hydrocyclones*, https://www.sciencedirect.com/science/article/pii/S0892687599001648, 2000. Accessed: 29.10.18

[20] Dr. John Walsh, *Selection and Troubleshooting of Flotation Equipment for Produced Water Handling*, http://petrowatertech.com/wp-content/uploads/2015/08/Flotation-Webinar29Nov2012-21.pdf, 2012. Accessed: 29.10.18

[21] The Engineering Toolbox, https://www.engineeringtoolbox.com/gas-density-d_158.html. Accessed: 01.10.18

[22] Keith Dunaway , *Collision Frequency*, https://chem.libretexts.org/Textbook_Maps/Physical_and_Theoretical_Chemistry_Textbook_Maps/Supplemental_Modules_(Physical_and_Theoretical_Chemistry)/Kinetics/Modeling_Reaction_Kinetics/Collision_Theory/Collision_Frequency, 2017. Accessed: 29.10.18

[23] Genesis group, http://www.genesisny.net/Commodity/Oil/ODefinitions.html.Accessed: 01.10.18

[24] Christoph Josef Backi, *SUBPRO Business Cases - Field Characteristics and Design Data*, 20.05.16. Accessed: 27.08.18

[25] SPE Join, *Oil emulsions* https://petrowiki.org/Oil_emulsions, 2015. Accessed: 03.10.18

[26] Scott Jenkins, *CEPCI UPDATES: JANUARY 2018 (PRELIM.)*, https://www.chemengonline.com/cepci-updates-january-2018-prelim-and-december-2017-final/?printmode=1, Chemical Engineering Essential for the CPI professionals, March 19, 2018. Accessed: 10.10.18

[27] Schlumberger, https://www.glossary.oilfield.slb.com/en/Terms/r/retention_time.aspx. Accessed: 17.10.18

[28] PetroWiki, *Oil emulsions* https://petrowiki.org/Oil_emulsions, July 2015. Accessed: 17.10.18

[29] Oil and gas journal, *SUBSEA TECHNOLOGY: RISING TO THE CHALLENGES OF THE DEEP*, https://www.ogj.com/articles/print/volume-104/issue-8/supplement-to-oil-gas-journal/advances-in-subsea-technology/subsea-technology-rising-to-the-challenges-of-the-deep.html, 02/27/2006. Accessed: 04.10.18

[30] UTF, Underwater technology foundation https://www.utc.no/utf/om_subsea/subsea_technology/, 2018. Accessed: 07.10.18

[31] T. Husvega, O. Rambeaub ,T. Drengstiga, T. Bilstada, *Performance of a deoiling hydrocyclone during variable flow rates*,https://www.sciencedirect.com/science/article/pii/S089268750600313X, April 2007, Accessed: 22. 11.18

[32] D. R. Woods *Rules of Thumb in Engineering*, http://www.home-machine-shop.com/Rules_Thumb_Engineering.pdf, Vch Pub, 2007. Accessed: 17.10.18

[33] S.Aminib, D. Mowlaab, M. Golkarb. *Developing a new approach for evaluating a de-oiling hydrocyclone efficiency* https://www.sciencedirect.com/science/article/pii/S0011916411008393, January 2012, Accessed: 22.11.18

[34] Wikipedia, *Dissolved air flotation*, https://en.wikipedia.org/wiki/Dissolved_air_flotation, 11 January 2018. Accessed: 21.10.18

[35] DNV GL, Det Norske Veritas, *Recommended practice DNV-RP-F301 : Subsea separator structural design*, https://rules.dnvgl.com/docs/pdf/DNV/codes/docs/2007-04/RP-F301.pdf, April, 2007. Accessed: 17.11.18

[36] Rigzone, How Does Subsea Processing Work? https://www.rigzone.com/training/insight.asp?insight_id=327&c_id=. Accessed: 05.11.18

[37] J. Moreno-Trejo, T. Markeset, *Identifying Challenges in the Maintenance of Subsea Petroleum Production Systems*, https://link.springer.com/content/pdf/10.1007%2F978-3-642-33980-6_29.pdf, University of Stavanger, 2012.. Accessed:03.11.18

[38] Nazih Shammas, Gary F. Bennett, *Flotation Technology. Chapter: Separation of Oil from Wastewater by Air Flotation*, June 2010. Accessed: 29.10.18

[39] Dr M.Johns, *Solids Removal Grit Recovery by Hydrocyclone*, Meat and Livestock Australia Limited ,June 2008. Accessed: 07.11.18

[40] Dave Christophersen, *Veolia water solutions and technology*, http://www.veoliawatertech.com/crownsolutions/ressources/documents/2/21850,Issue-17-Flotation-DAF,IAF,SAF.pdf. Accessed: 11.11.18

[41] E24, Børs https://bors.e24.no/#!/instrument/C:PBROUSDBR%5CSP.IDCENE. Figure: KURSBILDET. Retrived: 22.November 2018. Accessed: 11.11.18

[42] Oilfieldwiki, *Subsea manifold*, 2016 http://www.oilfieldwiki.com/wiki/Subsea_manifold. Accessed: 11.11.18

[43] Intermoor, *How do suction piles work?* http://intermoorblog.com/how-suction-piles-work. Accessed: 11.11.18

[44] Oil states, *Subsea pipelines systems, PLEM/PLET Structures*, https://oilstates.com/subsea-pipeline-systems/deepwater/plem-plet-structures/.Accessed: 11.11.18

[45] Glen E. Lochte, Tony Kozel, *How pigging operations impact deepwater production economics*, 1995. Accessed: 11.11.18

[46] Hydrasun, *Flying Leads*, https://www.hydrasun.com/products-services/umbilicals-subsea-connectors/flying-leads/.Accessed: 11.11.18

[47] The Norwegian Society for Oil and Gas Measurement, *https://nfogm.no/wp-content/uploads/2014/02/MPFM*$_{H}andbook_{R}evision2_{2}005_{I}SBN - 82 - 91341 - 89 - 3$*.pdf*, $March$2005.$Accessed$: 11.11.18

[48] Oilfield wiki, *Subsea Umbilical Termination Assembly (SUTA)*, http://www.oilfieldwiki.com/wiki/Subsea_Umbilical_Termination_Assembly_(SUTA). Accessed: 11.11.18

[49] Rigzone, *How Do Subsea Trees Work?*, https://www.rigzone.com/training/insight.asp?insight_id=302&c_id=. Accessed: 11.11.18

[50] Investopedia, *PV10*, https://www.investopedia.com/terms/p/pv10.asp. Accessed: 11.11.18

[51] Norwegian Petroleum, https://www.norskpetroleum.no/en/economy/petroleum-tax/, 2018. Accessed: 18.11.18

[52] Nick K. Lioudis, *How do average costs compare among various oil drilling rigs?* https://www.investopedia.com/ask/answers/061115/how-do-average-costs-compare-different-types-oil-drilling-rigs.asp, February 27, 2018. Accessed: 18.11.18

[53] SINTEF, https://www.sintef.no/en/flow-assurance1/. Accessed: 18.11.18

[54] Petrowiki, https://petrowiki.org/Flow_assurance_for_offshore_and_subsea_facilities, *Flow assurance for offshore and subsea facilities*. Accessed: 18.11.18

[55] Oil Price, https://oilprice.com/oil-price-charts/51. Accessed: 18.11.18

[56] E24, https://e24.no/. Accessed: 18.11.18

[57] NORSOK, http://www.standard.no/pagefiles/1176/m-001.pdf. Accessed: 18.11.18

[58] Sandvik, https://www.materials.sandvik/en/materials-center/material-datasheets/tube-and-pipe-seamless/sandvik-saf-2205/. Accessed: 18.11.18

[59] T. Frankiewicz, C.M Lee, K. Juniel, Compact Induced Gas Flotation As An Effective Water Treatment Technology On Deep Water Platforms, https://www.researchgate.net/publication/254518862_Compact_Induced_Gas_Flotation_As_An_Effective_Water_Treatment_Technology_On_Deep_Water_Platforms, Retrived: 22.November. Page 6, Table 1. Accessed: 19.11.18

[60] Matthew D. Stuber, Achim Wechsung, Arul Sundaramoorthy, Paul I. Barton, *Worst-Case Design of Subsea Production Facilities UsingSemi-Infinite Programming*, Massachusetts Institute of Technology, Cambridge, July 2014. Accessed: 22.11.18

[61] Mandar Thombre, Marlene Lund, Hanne Betten, *Subsea Separation*, Trondheim, 2015. Accessed: 27.08.18

[62] Gro Mogseth, Technical coordinator, Oral conversation: 03.11.18.

A Models

A.1 Gravitational separator

A.1.1 Simulation

The simulation of the three-phase gravity separator is based on the two-phase separator model from *Worst-Case Design of Subsea Production Facilities Using Semi-Infinite Programming*[60]. It was simulated by simplifying the separator as a two-phase (liquid-liquid) separator in an empirical model. This empirical model is only dependent on the residence time, the volume of the horizontal vessel, oil- and water-volumetric flows and the mass fraction of oil in the inflow. It also require a user specified performance constant.

In the two-phase separator, the rate of oil separation is given,

$$\frac{dx_o}{d\tau} = -k\tau \tag{2}$$

where k is the separator performance constant, and τ is the retention time. x_o is the outlet fraction of oil-in-water. The retention time is defined as the amount of time the liquid stays in a vessel. The retention time is calculated as,

$$\tau = \frac{V_v}{q_o + q_w} \tag{3}$$

where V_v is the volume of the vessel, q_o is the volumetric flow of oil and q_w is the volumetric flow of water. Solving equation 2 gives the simple exponential equation for the mass fraction of oil in the water outflow,

$$x_o = x_{o,in} exp[-k\tau] \tag{4}$$

where $x_{o,in}$ is the mass fractions of oil in the inflow.

A.1.2 Efficiency constant used in simulation

Table 30 gives the empirical constant used to calculate the separation efficiency[17]. The constant is user specified, and was chosen due to reasonable results and guidance.

Table 30: Gravity separator parameter.

k [-]	0.03

A.2 Hydrocyclone

A.2.1 Simulation

The hydrocyclone was simulated using an empirical model derived from experimental results published by Petro Water Tech[17]. The model is based on the particle cut size, d_{75}, which is the oil particle diameter were the hydrocyclone operates with an efficiency of 75%. An article published by L.R.Castilho and R.A.Medronho also used a similar model but with a cut size of 50%, but with empirical constants based on a solid-liquid hydrocyclone[19].

Figure 19 shows the correlation between the inlet Reynolds number and the hydrocyclone number, N_{Hy}.

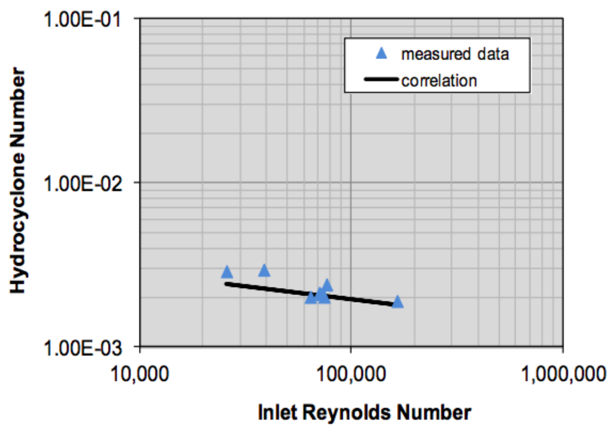

Figure 19: Correlation between hydrocyclone number and inlet Reynolds number[17].

Inlet Reynolds number is given by,

$$N_{RH_i} = \frac{\rho_{in} v_{in} D_{in}}{\mu} \tag{5}$$

where ρ_{in} is the inlet density, v_{in} is the inlet velocity, D_{in} is the inlet diameter and μ is the dynamic viscosity of water. The inlet density is approximated using the average between the two phases,

$$\rho_{in} = x_w \rho_w + x_o \rho_o \tag{6}$$

where x_w and x_o are respectively the mass fractions of water and oil.

The inlet velocity is given by,

$$v_{in} = \frac{4q_{in}}{\pi D_{in}^2} \tag{7}$$

where q_{in} is the volumetric flow at the inlet, which is found by dividing the total volumetric flow by the average number of required liners.

The hydrocyclone number can then be approximated from Figure 19 and is given as,

$$N_{Hy} = \frac{q\Delta\rho d_{75}^2}{\mu D_c^3} \tag{8}$$

where $\Delta\rho$ is the density difference between water and oil, D_c is the body diameter of the hydrocyclone and d_{75} is a parameter describing the drop diameter for which 75% of the drops are separated.

From d_{75}, the migration probability can be calculated trought the empirical formula,

$$M_p(d) = 1 - e^{c_3(\tilde{d_{75}} - c_4)^{c_5}} \tag{9}$$

where $\tilde{d_{75}}$ is the reduced drop diameter and c_3, c_4 and c_5 are empirical constants. The migration probability is the probability for an oil particle to migrate to the core of the hydrocyclone, which is equivalent to the separation efficiency.

The reduced drop diameter is defined as,

$$\tilde{d_{75}} = \frac{d}{d_{75}} \tag{10}$$

where d is the drop diameter. The fraction out of the hydrocyclone can then be calculated from the bubble distribution, $y(d)$, given,

$$x_{out} = \sum_{d=1}^{150} y(d)(1 - M_p(d)) \tag{11}$$

A.3 Induced Gas Flotation

A.3.1 Simulation

The efficiency of oil removal is primarily a function of the probability of collision between a gas bubble and oil droplet. As a basis to determine the collision frequency a simple system with only one moving gas bubble in the tank was modelled. An illustration of this process is shown in Figure 20. Assuming that the gas bubble has a one dimensional trajectory moving upwards in the tank, the collisions frequency for a single gas bubble is given as[22],

$$Z_g = \frac{V_{col}\rho_{b,o}}{\Delta t} \tag{12}$$

where V_{col} is the volume of the collision cylinder, $\rho_{b,o}$ is the density of oil bubbles in the tank and Δt is the time interval. The unit for Z_g is the number of collisions for one gas bubble over the density of oil bubbles per unit time.

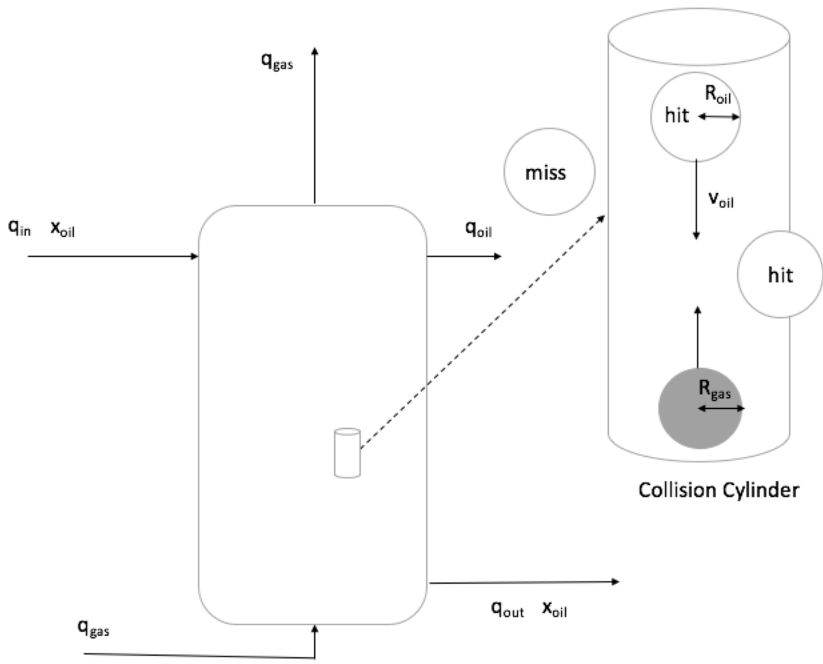

Figure 20: Illustration of the principle of a collision cylinder in a flotation tank.

The volume of the collision cylinder is given as[22],

$$V_{col} = \pi(r_g^2 + r_o^2)v_{rel}\Delta t \tag{13}$$

As the equation is sourced from an article based on gas collision, there was made a modification. The Equation 13 is originally multiplied with $\sqrt{2}$ to account for the fact that collisions might occur in from all directions, but as motion of the bubbles in the flotation tank mainly will be one directional, this term was omitted. r_o and r_g are the radius of oil and gas bubbles and is assumed to be constant. v_{rel} is the relative velocity. Because of the counter current flow of oil and gas, the relative velocity will be the sum of the individual flows,

$$v_{rel} = v_o + v_g \tag{14}$$

where v_o and v_g are respectively the velocity of oil and gas. As the oil follows the bulk flow of the inlet stream the velocity will be given by,

$$v_o = \frac{q_o}{A} \tag{15}$$

where A is the area of the tank, and q_o is the volumetric flow rate of oil. The velocity of gas bubbles will rise according to stokes law[13],

$$v_g = \frac{2}{9}\frac{(\rho_w - \rho_g)r_o^2 g}{\mu} \tag{16}$$

where μ is the dynamic viscosity of water and g is the gravity constant.

To account for all the collisions in the tank, Equation 12 is multiplied by the gas bubble density, $\rho_{b,g}$ as well as multiplying by a factor of $\frac{1}{2}$ to avoid counting each collision twice[22],

$$Z_{g,o} = \frac{1}{2}Z_i\rho_{b,g} \tag{17}$$

Inserting Equation 17 into 12 yields the equation for the total number of collisions in the flotation unit,

$$Z_{g,o} = \frac{1}{2}\pi(r_o^2 + r_g^2)v_{rel}\rho_{b,g}\rho_{b,g} \tag{18}$$

However, a collision between a oil and a gas particle does not necessary result in capture. To account for this, the equation is multiplied by the capture efficiency, E, which describes the number for how many of the collisions result in attachment[20],

$$Z_{g,o} = E\frac{1}{2}\pi(r_o^2 + r_g^2)v_{rel}\rho_{b,g}\rho_{b,g} \tag{19}$$

Equation 19 will be the basis for describing the the number of gas-oil attachments per unit second.

B Size estimation of equipment

B.1 Gravity separator

The size of the horizontal three-phase gravity separator is calculated following the procedure for a horizontal two-phase gravity separator in *Chemical engineering design*[16]. An illustration of a horizontal two-phase separator is shown Figure 21.

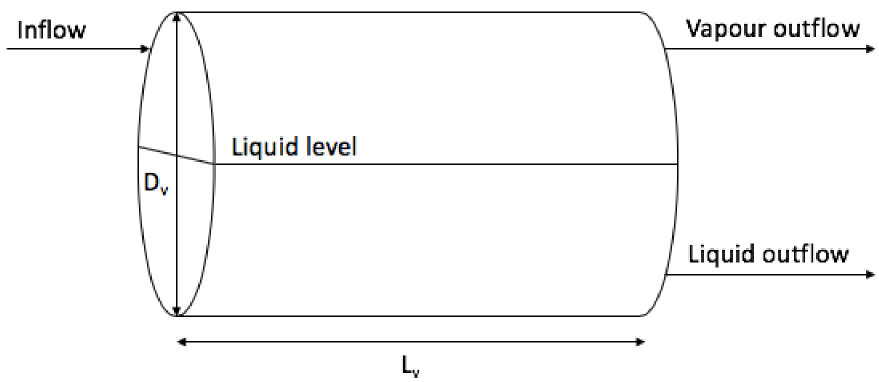

Figure 21: Horizontal two-phase separator.

The settling velocity, u_t, of the liquid droplets is calculated by

$$u_t = 0.07\left(\frac{\rho_l - \rho_v}{\rho_v}\right)^{1/2} \tag{20}$$

where ρ_l is the liquid density and ρ_v is the vapour density.

If the vessel does not have a demister pad,

$$u_s = 0.15u_t \tag{21}$$

where the factor provides a margin of safety and allows flow surges.

The vessel diameter in the horizontal separator is dependent of the length. The separator requires a sufficient vapour residence time for the liquid droplets to settle out, and a determined liquid hold up time. The diameter, length and the liquid level must therefore be chosen to fulfil these requirements. The most economical ratio between the length and diameter will depend on the operating pressure. The relation between the length, L_v, to the diameter, D_v, ratio and the operational pressure are given in Table 31.

Table 31: The relation between the length to diameter ratio and the operational pressure.

Operating pressure [bar]	$\frac{L_v}{D_v}$
0 - 20	3
20 - 35	4
>35	5

The operational pressure in the separator in this case is >35 bar, which leads to $\frac{L_v}{D_v}$ = 5.

The liquid height, h_v, can be calculated by,

$$h_v = f_v D_v \tag{22}$$

where f_v is the fraction of the total cross sectional area occupied by the vapour. The fraction is assumed to be half of the vessel, f_v = 0.5. This is inconsistent with the GOR, but is sufficient for preliminary designs.

The cross sectional area for vapour flow is given by,

$$A_c^v = \frac{\pi D_v^2}{4} \cdot f_v \tag{23}$$

The vapour velocity is given,

$$v_v = \frac{q_v}{A_c^v} \tag{24}$$

where q_v is the volumetric flow rate of vapour.

Vapour residence time, τ_v, required for the droplets to settle to liquid surface is given,

$$\tau_v = \frac{h_v}{u_s} \tag{25}$$

Actual residence time is given by,

$$\tau_{act} = \frac{L_v}{v_v} \tag{26}$$

For a separation which is satisfied, the actual residence time is equal to the required vapour residence time,

$$\tau_{act} = \tau_v \tag{27}$$

Solving equation 27, gives the vessel diameter, D_v. Now that the diameter is known, the length of the vessel can be found from the ratio between the length and diameter.

Liquid cross sectional can be calculated by,

$$A_c^l = \frac{\pi D_v^2}{4} \cdot (1 - f_v) \tag{28}$$

The liquid hold-up volume is given by,

$$V_h = A_c^l L_v \tag{29}$$

and the liquid hold-up time is given by,

$$t_h = \frac{V_h}{q_l} \tag{30}$$

where q_l is the volumetric flow rate of liquid.

Liquid hold-up time is required to be minimum 3 min[27]. If the hold-up time is lower than 3 min, the liquid hold-up volume has to be increased by increasing the vessel diameter. This can be done by calculating the diamter with the factor

$$f = \left(\frac{10}{t_h}\right)^{f_v} \tag{31}$$

The new vessel diameter is then multiplied with the factor, f, and a new liquid hold-up time is found. The calculations continues until the hold-up time is satisfied.

B.2 Hydrocyclone

B.2.1 Sizing and droplet distribution

According to Rietema[19], the geometric relationships in a hydrocyclone is derived from the body diameter, D_c, as shown in Figure 22.

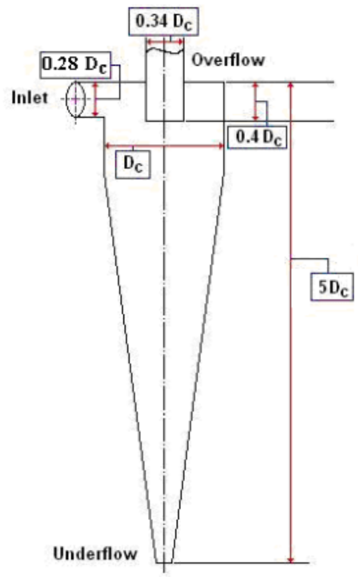

Figure 22: Geometric relationship in hydrocyclone.

Choosing the geometry is necessary for obtaining the optimal separation efficiency. A small inlet diameter will result in a higher radial velocity thus creating more force and a greater separation. However, a small inlet diameter also require more liners. The diameter of the early deoiling hydrocyclones were typically around 120 mm and was therefore able to treat large capacities, but had a lower separation efficiency. However, modern hydrocyclones usually have a diameter ranging from 40 to 50 mm bundled together into a single vessel to provide the same capacity[18].

Hydrocyclones are configured in a way where it is easy to install more liners when the flow rates increase[17]. However, installing more liners would add a significant cost as the hydrocyclones will be located subsea. As seen in Figure 23, the inlet needs a certain minimum and maximum flow to maintain a high efficiency. As the flow rates will change during the lifespan of the oilplant, the optimal number has to lie in a range which fulfils the condition for a certain flow rate. There are two limiting cases which determines the number of liners; the year which yields the smallest liquid production, and the years which gives a largest liquid production.

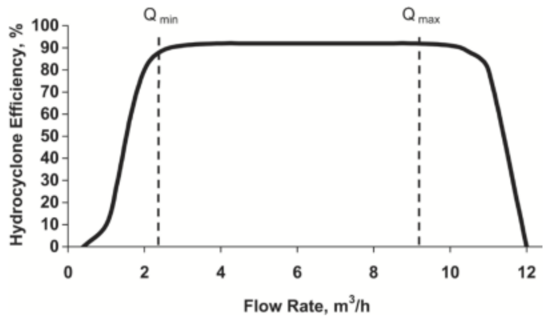

Figure 23: Hydrocyclone efficiency as a function of inlet flow rate[17].

The number of liners was found by dividing the total inflow from the gravity separator by the maximum and minimum flow rate as shown in Figure 23.

Table 32: Minimum and maximum liners to obtain desired efficiency for year 2 and 21.

Case	flow rate [$\frac{m^3}{h}$]	Min liners	Max liners
Minimum liquid production	134.6	15	64
Maximum liquid production	361	40	172

To meet the minimum and maximum inlet flow rate requirement for every year, this hydrocyclone require between 40 and 64 liners.

B.2.2 Inlet Distribution

After the gravity separator, the oil fraction will mainly be an emulsion of oil in water. As the efficiency hydrocyclone will vary depending on the radius of the oil particles, a simple distribution was established. Emulsions normally have a droplet size range that can be represented by a distribution function, as shown in Figure 24. The distribution will vary depending on the presence of solids, bulk properties of oil and water, and natural occurring emulsifying agents, but is neglected when establishing the emulsion.[25].

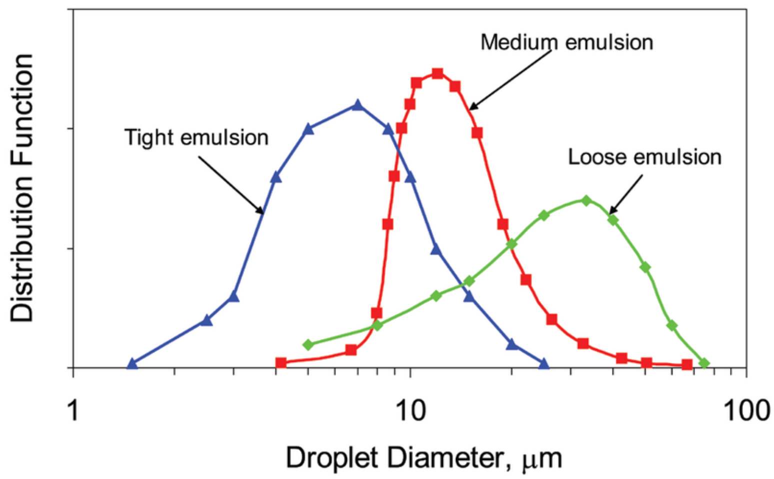

Figure 24: Distribution of droplet diameters in an oil emulsion[25].

As a simplification it was assumed that til emulsion follows a normal distributed function, y(d), with the radius ranging from 1μm to 150μm, with expected value, $\bar{x}$, equal to the average value, and standard deviation, σ, equal to 30μm, to imitate the distribution curve from Figure 24. The distribution was corrected relative to the mass fraction, so that the sum of all the fraction would equal the total oil fraction.

$$\sum_{x=1}^{N} y(D = d, \bar{x}, \sigma) = x_o \tag{32}$$

B.2.3 Efficiency constants used in simulation

Table 33 gives the empirical constants used to calculate the separation efficiency[17].

Table 33: Hydrocyclone parameters.

c_3 [-]	-1.2
c_4 [-]	0.35
c_5 [-]	0.3

B.3 Flotation

B.3.1 Sizing and design parameters

To achieve the desired outlet concentration, the inlet bulk flow needs to have a certain residence time in the tank. To fulfil this condition the height of the tank can roughly be approximated as,

$$H = v_b \tau \tag{33}$$

where v_b is velocity of the oil water bulk flow, and τ is the required residence time for separation. By assuming one dimensional flow in the tank, v_b can be found by,

$$v_b = \frac{q_b}{A} \tag{34}$$

where q_b is the volumetric bulk flow, and A is the cross sectional area.

Petro Water Tech published guidelines, shown in Table 34, for selecting key parameters for a flotation unit. All dimensions and sizes will therefore be within these ranges.

Table 34: Commercial available maximum and minimum values for flotation units[20].

	min	max
Residence time [sec]	30	240
Height/Width Rato[-]	1	4
Gas bubble size [μm]	30	1200

B.3.2 Residence time and height

Finding the optimal residence time will be directly related the height of the unit. A larger residence time will consequently lead to higher degree of capture in the tank, but will accordingly require a larger column height. These values were selected from the limiting cases which is at the start of the lifespan, which yields a low bulk flow and a high oil inlet concentration and at the end when the bulk flow is large but the inlet concentration is low. As the water stream increases, the bulk flow velocity in the tank also increases which decreases the overall residence time. However, since because of the inlet concentration is lower, the requirement for residence will also decrease.

Increasing the radius in the tank could be a solution for increasing the residence time. However, this would also require a larger gas stream to obtain a high concentration of gas bubbles. The gas bubbles also needs to be kept uniformly distributed in the tank which could be harder with an increasing radius.

By trial and error the year for maximum liquid production and maximum oil content, required a minimum height of 2 meters and a radius of 0.5 meter to yield an outlet oil concentration under 30ppm.

To what extent the calculated dimensions will match realistic values is questionable. The assumption of one dimensional flow without any turbulence gives an unrealistic picture. In reality the flow path will be highly irregular which would also increase the actual residence time. The calculated height of the flotation tank could therefore be an overestimation.

B.3.3 Gas parameters

As the production facility will be located subsea accessing gas from air or gas tanks will be inconvenient. Instead, the produced natural gas will be utilised as the gas source. Because of the large gas-oil ratio, access to the gas stream is assumed to be unlimited.

The efficiency of the flotation unit will vary with the radius of the oil and gas radius. When large gas bubbles, approximately 700 microns, are used, the capture efficiency is roughly 1 in 10,000. In contrast, small gas bubbles yields a capture efficiency of 1 in 100[20]. The large deviation is a result of the fact that large gas bubbles rise faster and create more swirl around their path, and the oil drops tend to dodge the gas bubbles and follow the streamlines instead[20]. The black line in Figure 25 shows the correlation between capture efficiency and gas bubble diameter without chemicals and will be used as a basis to determine the capture efficiency.

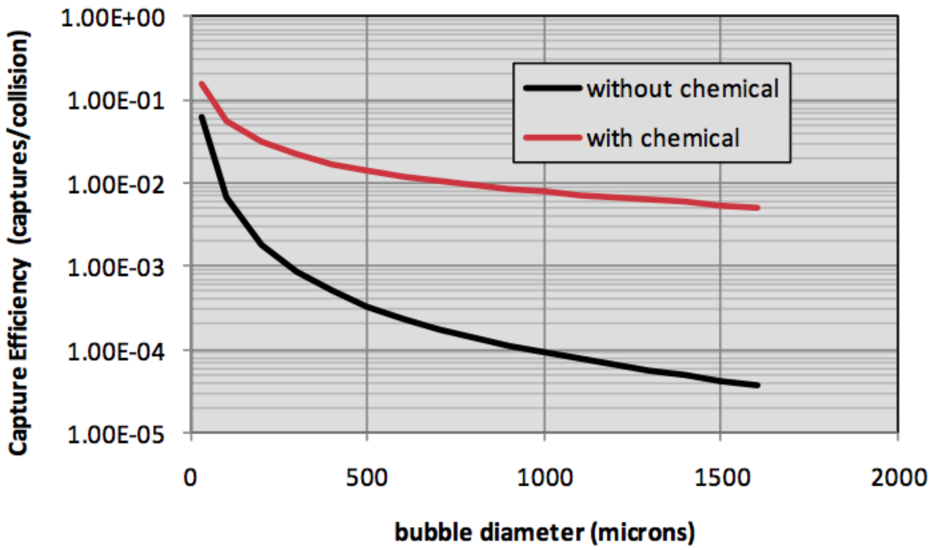

Figure 25: Capture efficiency as a function of gas diameter[20].

Different flotation devices will produce different gas bubble sizes. A large gas flow with small bubbles will according to the model yield the highest collision frequency. Due to the high cost of generation small bubbles, no machine can produce both small bubbles and a lot of gas[20]. The alleged gas size varied from every source. As shown i Table 34 the range for available gas sizes is wide. However, other sources claimed that the average bubble sizes usually lied within the range of 80 and 300 microns[38], while others just claimed it to be from 70 microns and larger[40]. Due to disagreement between the sources, an average value of 400 microns with a corresponding capture efficiency of $\frac{1}{1000}$ is chosen for the simulation.

An experiment investigating deoiling gas flotation units conduced by R.Mastouri1, S.M. Borghei, F.Nadim, and E.Roayaei supplied a flotation tank with a volume of 14.8L a pure nitrogen gas feed of $10\frac{L}{min}$,and achieved a separation efficiency of 80%[12]. Making preliminary estimates, the volume required to handle the inlet stream from the oil reservoir is approximately $2m^3$. Scaling the gas feed to obtain the correct dimensions requires a gas stream of approximately 1.2 $\frac{m^3}{min}$, or 0.02$\frac{m^3}{s}$. However, since inlet oil concentration investigated in the experiment was 300ppm, which is 6 times larger than this flotation device averagely has to process, the required gas stream might be less than 0.02$\frac{m^3}{s}$.

B.3.4 Oil parameters

Just as in the hydrocyclone, the performance in flotation will depend on the inlet drop distribution. Larger oil bubbles would increase the probability of collision, but also resulting in a lower bubble density. However as previously mentioned, larger bubbles will generally create more turbulence, hence decrease the capture efficiency.

As the model do not take this into account the average oil droplet size was calculated from the outlet distribution of the hydrocyclone.

C Case data

The case data shown below are the simulations results based on the three models for the separations. The water production at year one is equal to zero, so the water treatment is not necessary this year. Therefore, year one is not included in the simulations.

C.1 Case 1

Table 35 includes the values for all the volumetric flows with corresponding mass fraction of oil, for the project from year 2-10. q_0 is the volumetric flow out of the reservoir, q_1 is the volumetric flow out of the gravity separators, q_2 is the outlet volumetric flow from the hydrocyclone, and q_3 is the outlet volumetric flow from the induced gas flotation unit. The volumetric flows have corresponding mass fractions of oil, respectively x_0, x_1, x_2 and x_3.

Table 35: Volumetric flow, $q_i[\frac{m^3}{s}]$, with corresponding mass fraction, x_i[-], for year 2-10 for case 1.

Year	q_0	q_1	q_2	q_3	x_0	x_1	x_2	x_3
2	0.0720	0.0044	0.0031	0.0029	0.9598	0.3398	0.0672	0.0113
3	0.0914	0.0171	0.0110	0.0107	0.8861	0.3913	0.0516	0.0237
4	0.1088	0.0459	0.0300	0.0297	0.7340	0.3693	0.0349	0.0272
5	0.1238	0.0704	0.0476	0.0474	0.6262	0.3424	0.0276	0.0238
6	0.1285	0.0791	0.0546	0.0544	0.5856	0.3273	0.0252	0.0222
7	0.1285	0.0835	0.0592	0.0591	0.5495	0.3071	0.0232	0.0206
8	0.1273	0.0872	0.0638	0.0637	0.5091	0.2830	0.0210	0.0189
9	0.1250	0.0901	0.0684	0.0683	0.4630	0.2546	0.0187	0.0169
10	0.1215	0.0922	0.0729	0.0728	0.4095	0.2214	0.0161	0.0146

C.2 Case 2

Table 36 includes the values for all the volumetric flows with corresponding mass fraction of oil, for year 2-10. q_0 is the volumetric flow out of the reservoir, q_1 is the volumetric flow out of the gravity separators, q_2 is the outlet volumetric flow from the first hydrocyclone, and q_3 is the outlet volumetric flow from the second hydrocyclone. The volumetric flows have corresponding mass fractions of oil, respectively x_0, x_1, x_2 and x_3.

Table 36: Volumetric flow, $q_i[\frac{m^3}{s}]$, with corresponding mass fraction, x_i[-], for year 2-10 for case 2.

Year	q_0	q_1	q_2	q_3	x_0	x_1	x_2	x_3
2	0.0720	0.0044	0.0031	0.0029	0.9598	0.3398	0.0672	0.00158
3	0.0914	0.0171	0.0110	0.0105	0.8861	0.3913	0.0516	0.0084
4	0.1088	0.0459	0.0300	0.0291	0.7340	0.3693	0.0349	0.0043
5	0.1238	0.0704	0.0476	0.0464	0.6262	0.3424	0.0276	0.0030
6	0.1285	0.0791	0.0546	0.0534	0.5856	0.3273	0.0252	0.0026
7	0.1285	0.0835	0.0592	0.0580	0.5495	0.3071	0.0232	0.0024
8	0.1273	0.0872	0.0638	0.0626	0.5091	0.2830	0.0210	0.0021
9	0.1250	0.0901	0.0684	0.0673	0.4630	0.2546	0.0187	0.0019
10	0.1215	0.0922	0.0729	0.0719	0.4095	0.2214	0.0161	0.0016

C.3 Case 3

Table 37 includes the values for all the volumetric flows with corresponding mass fraction of oil, for year 2-10. q_0 is the volumetric flow out of the reservoir, q_1 is the volumetric flow out of the gravity separators, q_2 and q_3 are the outlet volumetric flows from respectively the first and second induced gas flotation units. The volumetric flows have corresponding mass fractions of oil, respectively x_0, x_1, x_2 and x_3.

Table 37: Volumetric flow, $q_i[\frac{m^3}{s}]$, with corresponding mass fraction, x_i[-], for year 2-10 for case 3.

Year	q_0	q_1	q_2	q_3	x_0	x_1	x_2	x_3
2	0.0720	0.0044	0.0029	0.0029	0.9598	0.3398	0.0000	0.0000
3	0.0914	0.0171	0.0104	0.0104	0.8861	0.3913	0.0000	0.0000
4	0.1088	0.0459	0.0301	0.0290	0.7340	0.3693	0.0386	0.0007
5	0.1238	0.0704	0.0511	0.0469	0.6262	0.3424	0.0948	0.0139
6	0.1285	0.0791	0.0599	0.0545	0.5856	0.3273	0.1118	0.0228
7	0.1285	0.0835	0.0652	0.0595	0.5495	0.3071	0.1126	0.0269
8	0.1273	0.0872	0.0698	0.0644	0.5091	0.2830	0.1046	0.0289
9	0.1250	0.0901	0.0746	0.0692	0.4630	0.2546	0.1003	0.0300
10	0.1215	0.0922	0.0786	0.0740	0.4095	0.2214	0.0876	0.0299

D Cost estimation

D.1 Methods for cost estimation

For the different phases in the project, there are different methods to perform the cost estimation. The cost estimation also depends on the amount of data and resources available. Two different methods for cost estimation are: cost-capacity estimation and factorial estimation. The first method, cost-capacity estimation, has a $\pm$30 $\%$ accuracy range, and is based on an estimation of the order-of-magnitude. With knowledge of costs of earlier projects with the same manufacturing process, an estimate of the cost can be made by,

$$C_1 = C_0\Big(\frac{S_2}{S_1}\Big)^n = aS_2^n \tag{35}$$

where C_1 and C_0 is the ISBL cost of the plants with capacities S_2 and S_1. The exponential cost factor, n, varies from process to process, and usually take a value between 0.5 and 0.9. An average in the whole chemical industry is n= 0.6. a is a cost constant[15].

The factorial method is based on an estimate of the purchase cost of the major required equipment for the project, while the rest of the costs are being estimated as factors of the cost of equipment. This method also has an accuracy of $\pm$30 $\%$. A quick estimate of the fixed capital costs is given by,

$$C = F\Big(\sum C_e\Big) \tag{36}$$

where C is the total plant ISBL capital cost, $\sum$C$_e$ is the total delivered cost of all major equipment and F is an installation factor, the ”Lang factor”, and is dependent of process type.

For more accurate estimates, one can take out the different individual factors from the ”Lang factor”. Typical factors that are included in this estimation can be equipment erection, piping, instrumentation and control, electrical, civil and structures and buildings and lagging’s and paint. The total capital cost can then be estimated by,

$$C = \sum_{i=1}^{i=M} C_{e,i,CS}[(1+f_p)f_m + f_{er} + f_{el} + f_i + f_c + f_s + f_l] \tag{37}$$

or

$$C = \sum_{i=1}^{i=M} C_{e,i,A}[(1+f_p) + (f_{er} + f_{el} + f_i + f_c + f_s + f_l)/f_m] \tag{38}$$

where $C_{e,i,CS}$ and $C_{e,i,A}$ is the purchased carbon steel and alloy equipment cost of equipment i, and M is the total number of equipment. f_p is the installation factor for piping and f_m is the material factor defined as,

$$f_m = \frac{purchased\ cost\ of\ item\ in\ exotic\ material}{purchased\ cost\ of\ item\ in\ carbon\ steel} \tag{39}$$

f_{er}, f_{el}, f_i, f_c, f_s and f_l is the installation factors for respectively equipment erection, electrical work, instrumentation and process control, civil engineering work, structures and buildings and installation lagging, insulation and paint. There will also be an extra installation factor for subsea construction, f_{sub}[15], which is assumed to be 3. The installation factors are given in Table 38.

Table 38: Installation factors used in the cost calculations.

Factor	Value
f_{er}	0.3
f_p	0.8
f_i	0.3
f_{el}	0.2
f_c	0.3
f_s	0.2
f_l	0.1
f_m	1.56
f_{inst}	4.208
f_{sub}	3

D.2 Estimating purchased equipment cost

The purchased equipment costs are the basis of the factorial method of cost estimation. It is therefore necessary to have good estimates for the equipment costs. For preliminary estimates the purchased equipment cost on a US Gulf Coast basis (2007), is given,

$$C_0 = a + bS^n \tag{40}$$

where a and b are cost constants, S is the size parameter and n is the exponent for that type of equipment. Multiplying with the two installation factors, gives the final cost,

$$C_1 = C_0 f_{sub} f_{inst} \tag{41}$$

D.3 Cost-driving factors

When estimating cost of materials and labour, inflation must be considered. The historical cost data used to estimate cost has to be updated with the use of published cost indices. The cost indices are based on data for material, labour and energy costs and is to be found in government statistical digests. The cost estimation in the desired year is given by

$$C_2 = \frac{I_2}{I_1} C_1 \tag{42}$$

where C_2 is the cost in the desired year, C_1 is the cost in the cost for the historical data. I_2 is the cost index in the desired year, and I_1 is the cost index for the historical data[15].

D.4 Material

All the equipment installed subsea is assumed to be made of 22 Cr duplex stainless steel(2205). This is recommended because the metal is robust and resistant to corrosion. Properties for the chosen material are given in Table 39[57].

Table 39: Properties of the material 22 Cr duplex stainless steel.

Property	
Composition [57]	22% Cr, 5.5% Ni, 3% Mo
Density [58]	7800 $\frac{kg}{m^3}$
Cost	1.56 $\cdot$f$_{carbon\ steel}$

D.5 Separator

To estimate the cost of the separator, the shell mass needed to produce it had to be calculated. Shell mass is given by,

$$Shell\ mass = \pi D_v L_v t_w \rho_m \tag{43}$$

where D_v is the vessel diameter, L_v is the vessel length, t_w is the wall thickness and ρ_m is the metal density. The minimum required wall thickness is based on the relation between the water depth and the external allowable pressure[35]. The wall thickness is estimated to be 60mm.

The variables, describing the size of the vessel, used in the cost estimation is shown in Table 40.

Table 40: Variables, of the separator size, needed in the cost estimation.

Property	Value	Unit
t_w	60	mm
ρ_m	7800	kg/m^3
Shell mass	15 863.87	kg

The values of the parameters, in Equation 40, in the cost estimation are shown in Table 41.

Table 41: Cost data for the separator.

Equipment	unit for size, S	a [-]	b [-]	n[-]	C_0 [USD]
Horizontal pressure vessel, ss	Shell mass [kg]	11 000	63	0.85	245 255

The total equipment cost for the separator is then multiplied with the two factors and scaled accordingly to the CEPCI 2018 index.

Table 42: Cost data for the separator, scaled accordingly the CEPCI 2018 index.

C_0 [USD]	f_{inst}	f_{sub}	I_{2007} [-]	I_{2018} [-]	C_2 [USD]
245 255	4.208	3	509.7	591.33	3 591 944

D.6 Hydrocyclone

The cost estimation for the hydrocyclone takes basis in historic cost data given in table 43[32]. The final cost includes equipment erection, electrical work, instrumentation and process control, civil engineering work, structures, lagging, insulation, paint and testing. Table 43 shows the scaling and the cost estimation, where C_0 is the reference cost, and S is the size parameters given as the inlet flow rate in $\frac{L}{s}$. S_2 represents the case for maximum liquid flow.

Table 43: Cost data for the hydrocyclone.

C_0 [USD]	S_1 [$\frac{L}{s}$]	S_2 [$\frac{L}{s}$]	n[-]	$I_{reference}$ [-]	I_{2018} [-]	C_2 [USD]
38000	50	100.27	0.35	1000	591.33	367 880

Due to the relative low cost compared to the other units, the estimation was also compared to different historical costs. A beef processing facility published purchase and instalment costs for a more robust hydrocyclone closely related to deoiling hydrocyclones used in the industry[39]. The instalment cost includes material costs, supporting structure and piping etc. The hydrocyclone also has the same design flow($300 m^3/h$). Scaling in terms of material costs, CEPCI and subsea factor is presented in the Table 44.

Table 44: Cost data for the hydrocyclone, scaled accordingly the CEPCI 2018 index.

C_1 [USD]	$I_{reference}$ [-]	I_{2018} [-]	C_2 [USD]
104 000	575.4	591.33	500 194

Cost data on the basis of the body diameter was also available and analysed[32]. Since the data is based on a single liner, the number of liners will be crucial for the final instalment cost. Scaling in terms of the instalment factors, number of liners and from the values yields the cost estimations shown i Table 45.

Table 45: Cost data for the hydrocyclone, scaled accordingly the CEPCI 2018 index.

Liners	C_0 [USD]	S_1 $[cm]$	S_2 $[cm]$	n[-]	$I_{reference}$ [-]	I_{2018} [-]	C$_2[USD]$
40	6000	25	7.5	1.07	1000	591.33	502 488
52	6000	25	7.5	1.07	1000	591.33	653 234
64	6000	25	7.5	1.07	1000	591.33	803 981

The estimation based on the number of liners gave a more reasonable estimation compared to the first estimation based on the design flow. Due to the fact that the hydrocyclone might need spare liners that can work as a buffer in the case of clogging or maintenance, the cost estimation for 64 liners is used for further calculations.

D.7 Induced Gas Flotation unit

Scaling in terms of surface area, CEPCI, presented in Table 46, as well as the instalment factors and subsea factor, yields the final cost estimation C_2.

Table 46: Cost data for the induced gas flotation unit, scaled accordingly the CEPCI 2018 index.

C_0[USD]	S_1 $[m^2]$	S_2 $[m^2]$	n [-]	$I_{reference}$ [-]	I_{2018} [-]	C_2[USD]
500 000	20	7.85	0.48	1000	591.33	2 381 208

D.8 Flowline and riser

The equipment cost for flowline and riser are estimated by

$$C = f_t f_{size} C_0 L + C_{misc} L \tag{44}$$

where f_t is the flowline type factor, f_{size} is the size factor, C_0 is the basis cost per unit length, C_{misc} is the miscellaneous cost associated with the flowlines and L is the total length of the pipelines.

The pipeline, transporting oil and gas to the FPSO, is set to be 12inches (0.3048m). The flowline is assumed to be rigid, while the riser is assumed to be flexible.

Table 47: Cost data for the flowline and riser.

Type	Length [m]	Size [m]	f_t [-]	f_s[-]	$C_0[\frac{USD}{m}]$	C_{misc} [$\frac{USD}{m}$]	C_0 [USD]
Oil and gas flowline	150 000	0.3048	Rigid	1.30	230	500	119 850 000
Oil and gas riser	510	0.3048	Flexible	1.30	230	500	407 490
Total cost							**120 257 490**

The final, total cost for the flowline and the riser is scaled accordingly to the CEPCI 2018 index, and is given in Table 48.

Table 48: Cost data for the pipeline, scaled according to the CEPCI 2018 index.

C_0[USD]	$I_{2007}[-]$	$I_{2018}[-]$	C_2 [USD]
120 257 490	525.4	591.33	135 348 043

D.9 Umbilical

The cost for the umbilical includes electrical power cables, signal cables and conduits for hydraulic control fluid. The final cost is scaled accordingly to the CEPCI 2018 index. The cost data is shown in Table 49.

Table 49: Cost data for the umbilical, scaled accordingly the CEPCI 2018 index.

Type	Length [m]	C_0 [USD]	I_{2007} [-]	I_{2018} [-]	C_2 [USD]
Umbilical	150 510	229 254 363	525.4	591.33	258 022 426

D.10 Subsea Hardware

The cost for the individual hardware types and the total cost were scaled accordingly the CEPCI 2018 index and are shown in Table 50.

Table 50: Hardware cost, scaled accordingly the CEPCI 2018 index.

Hardware Type	Quantity	C_1 [USD]	$I_{reference}$ [-]	C_2 [USD]
Suction Pile	1	1 000 000	525.4	1 125 485
Production PLET	2	3 468 368	525.4	3 903 597
Production Tree Jumpers	3	975 174	525.4	1 097 544
Pigging	1	431 555	525.4	485 708
Production PLET Jumpers	2	1 796 872	525.4	2 022 353
Multiphase Flow Meter	1	924 250	525.4	1 040 229
Flying Leads	-	1 247 031	525.4	1 403 515
Sum				**11 078 413**

D.11 Control equipment

The cost for the individual control equipment and the total cost were scaled accordingly the CEPCI 2018 index and are shown in Table 51.

Table 51: Control equipment, scaled accordingly the CEPCI 2018 index.

Equipment	C_1 [USD]	Quantity	$I_{reference}$ [-]	C_2 [USD]
Topside control	2 967 704	-	525.4	3 340 107
Tree-Mounted control	5 108 940	3	525.4	5 750 037
SUTA	2 764 804	1	525.4	3 111 764
Sum				**12 201 908**

D.12 Testing cost

The individual cost for testing of equipment and the total cost were scaled accordingly the CEPCI 2018 index and are shown in Table 52.

Table 52: Testing cost, scaled accordingly the CEPCI 2018 index.

Equipment	C_1 [USD]	$I_{reference}$ [-]	C_2 [USD]
Subsea Hardware FAT,EFAT	27 132 162	525.4	30 536 850
Tree SIT and Commissioning	875 000	525.4	984 799
PLET SIT	565 499	525.4	636 460
Control System SIT	237 786	525.4	267 624
Sum			**32 425 733**

D.13 Engineering, Insurance and Contingency

The cost for engineering, insurance and contingency, and the total cost were scaled accordingly the CEPCI 2018 index and are shown in Table 53.

Table 53: Engineering, Insurance and Contingency costs, scaled accordingly the CEPCI 2018 index.

Type	C_1 [USD]	$I_{reference}$ [-]	C_2 [USD]
Engineering and Project Management Cost	4 738 427	525.4	5 333 030
Insurance	6 002 008	525.4	6 755 172
Contingency and Allowance	12 559 539	525.4	14 135 577
Sum			**26 223 779**

E Profitability Calculations

E.1 Cash Flows

The net income for a period i can be calculated from,

$$NI_i = R_i - OPEX_i \tag{45}$$

where R_i is the revenue of period i which is calculated as the sales income from the production of oil and gas. The fraction of oil that is left after the water treatment is neglected, so that the amount of oil and gas for sale are equal to the production rate from the reservoir. OPEX$_i$ is the operating expenditures for the period. CAPEX is not included in the net income, and is assumed to be an independent investment during the 0th period. The cash flow for the period i can then be calculated by subtracting the rate of taxation, t_r,

$$CF_i = NI_i(1 - t_r) \tag{46}$$

E.2 Net present Value (NPV)

The net present value of a project is the sum of the present values of the future cash flows, both positive and negative, and is given,

$$NPV = \sum_{n=1}^{n=t} \frac{CF_n}{(1+r)^n} \tag{47}$$

where CF_n is the cash flow in year n, t is the lifetime of the project and r is the interest rate.

Internal rate of return (IRR) is the project's effective depreciation, ie the interest rate that gives the net present value equal to 0.

$$0 = \sum_{n=1}^{n=t} \frac{CF_n}{(1+IRR)^n} \tag{48}$$

E.3 Pay-back time

Pay-back time is the time required to earn back the investment cost through the successive cash inflows. The pay-back time is given by,

$$t_{pb} = \frac{I}{CF_a} \tag{49}$$

where I is the total investment and CF_a is the average annual cash flow. The equation takes the assumption that all the investment is made in year zero and that the revenues begin immediately. In addition, the taxes and depreciation is not taken into account.

E.4 Return on investment (ROI)

Return on investment is percentage of investment that the annual cash flow represents, and is given by,

$$ROI = \frac{CF}{I} \cdot 100\% \tag{50}$$

where CF is the net annual cash flow.

F Matlab Scripts and simulations

F.1 Case 1

The following script was used to calculated all the outlet fractions and flows for case 1.

```
clear all
clc
close all
%**************** CASE 1 ***************%
% 1xgravity sep, 1xhydrocyclone, 1xflotation %

%% inlet conditions
q_0_oil = [5970 7000 6900 6700 6500 6100 5600 5000 4300 3600 3000 2500 2100 1750 1450 1200 1050 800 600 400];%[m3/d]
q_0_oil = q_0_oil./(3600*24);
q_0_w = [250 900 2500 4000 4600 5000 5400 5800 6200 6550 6900 7150 7400 7600 7800 7950 8100 8250 8400 8500];
q_0_w = q_0_w./(3600*24);
years = 1:1:20;
x_0 = zeros(1,length(years));
x_1 = zeros(1,length(years));
x_2 = zeros(1,length(years));
x_3 = zeros(1,length(years));
q_0 = zeros(1,length(years));
q_1 = zeros(1,length(years));
q_2 = zeros(1,length(years));
q_3 = zeros(1,length(years));
tau1 = zeros(1,length(years));


for i = 1:length(years)

x_0(i) = (q_0_oil(i))/(q_0_w(i) + q_0_oil(i));
q_0(i) = (q_0_oil(i) + q_0_w(i));

```

```
%% gravity separator
[x_1_a, q_1_a] = gravity_separator(x_0(i), q_0(i)/2); %x0: molefraxtion oil
    , q_0: oil,water volumetric flow
[x_1_b, q_1_b] = gravity_separator(x_0(i), q_0(i)/2); %x0: molefraxtion oil
    , q_0: oil,water volumetric flow

x_1(i) = x_1_a; %% assuming the two gravity separators have the same
    efficency, the outlet fraction will be the same for both.
q_1(i) = q_1_a + q_1_b; %% total liquid flow is the sum of the the two
    outlet flows

%% hydrocyclone

R_hyd = 150; %max range for distribution.

[x_2(i), q_2(i), avg_drop_size, num_liners_min, num_liners_max] =
    hydrocyclone(q_1(i), x_1(i), R_hyd);

%% flotation

gas_flow = 0.0033 % [m3/s]

[x_3(i), q_3(i), tau1(i)] = flotation_model(x_2(i), q_2(i), avg_drop_size,
    gas_flow);


end

years = 2:1:10;
figure()
plot(years, x_0(1:9), '*')
hold on
plot(years, x_1(1:9), '*')
hold on
plot(years, x_2(1:9), '*')
```

```
hold on
plot(years, x_3(1:9), '*')
hold on
plot(years, 0.03*ones(1,length(years)))
legend('x0, inlet from reservoir','x1, outlet gravity separator','x2,
    outlet hydrocyclone', 'x3, outlet IGF', '30 ppm')
xlabel('Time [year]')
ylabel('Oil fraction in waster water [-]')
title('Case 1: Oil fractions for year 2 to 10')

figure()
plot(years, q_0(1:9), '*')
hold on
plot(years, q_1(1:9), '*')
hold on
plot(years, q_2(1:9), '*')
hold on
plot(years, q_3(1:9), '*')
legend('q0, inlet flow from reservoir','q1, outlet flow gravity separator',
    'q2, outlet hydrocyclone', 'q3, outlet IGF', 'Location' ,'southeast')
xlabel('Time [year]')
ylabel('Flow [m3/s]')
title('Case 1: Liquid flows year 2 to 10')
```

F.2 Case 2

The following script was used to calculated all the outlet fractions and flows for case 2.

```

clc
clear all
close all
%*************** CASE 2 ***************%
% 1xgravity sep, 2xhydrocyclone %

```

```
q_0_oil = [5970 7000 6900 6700 6500 6100 5600 5000 4300 3600 3000 2500 2100
    1750 1450 1200 1050 800 600 400];%[m3/d]
q_0_oil = q_0_oil./(3600*24);
q_0_w = [250 900 2500 4000 4600 5000 5400 5800 6200 6550 6900 7150 7400
   7600 7800 7950 8100 8250 8400 8500];
q_0_w = q_0_w./(3600*24);
x_0 = zeros(1,length(years));
x_1 = zeros(1,length(years));
x_2 = zeros(1,length(years));
x_3 = zeros(1,length(years));
q_0 = zeros(1,length(years));
q_1 = zeros(1,length(years));
q_2 = zeros(1,length(years));
q_3 = zeros(1,length(years));
years = 1:1:20;

%% inlet conditions


for i = 1:length(years)

x_0(i) = (q_0_oil(i))/(q_0_w(i) + q_0_oil(i));
q_0(i) = (q_0_oil(i) + q_0_w(i));
q_oil = 0.0810; %[m^3/s]
q_water = 0.0104; %[m^3/s]

%% gravity separator

[x_1_a, q_1_a] =  gravity_separator(x_0(i), q_0(i)/2);
[x_1_b, q_1_b] =  gravity_separator(x_0(i), q_0(i)/2);
x_1(i) = x_1_a;
q_1(i) = q_1_a + q_1_b;



%% hydrocyclone
```

```
R_hyd = 150; % max range

[x_2(i), q_2(i), x_3(i), q_3(i)] = hydrocyclone_series(x_1(i), q_1(i));

end


years = 2:1:10;
figure()
plot(years, x_0(1:9), '*')
hold on
plot(years, x_1(1:9), '*')
hold on
plot(years, x_2(1:9), '*')
hold on
plot(years, x_3(1:9), '*')
hold on
plot(years, 0.03*ones(1,length(years)))
legend('x0, inlet from reservoir','x1, outlet gravity separator','x2,
    outlet first hydrocyclone', 'x3, outlet second hydrocyclone', '30 ppm')
xlabel('Time [year]')
ylabel('Oil fraction in waster water [-]')
title('Case 2: Oil fractions for year 2 to 10')

figure()
plot(years, q_0(1:9), '*')
hold on
plot(years, q_1(1:9), '*')
hold on
plot(years, q_2(1:9), '*')
hold on
plot(years, q_3(1:9), '*')
legend('q0, inlet flow from reservoir','q1, outlet flow gravity separator',
    'q2, outlet first hydrocyclone', 'q3, outlet second hydrocyclone', '
```

```
    Location' ,'southeast')
xlabel('Time [year]')
ylabel('Flow [m3/s]')
title('Case 2: Liquid flows year 2 to 10')
```

F.3 Case 3

The following script was used to calculated all the outlet fractions and flows for case 2.

```

clc
clear all
close all
%*************** CASE 2 ***************%
% 1xgravity sep, 2xhydrocyclone %

q_0_oil = [5970 7000 6900 6700 6500 6100 5600 5000 4300 3600 3000 2500 2100
    1750 1450 1200 1050 800 600 400];%[m3/d]
q_0_oil = q_0_oil./(3600*24);
q_0_w = [250 900 2500 4000 4600 5000 5400 5800 6200 6550 6900 7150 7400
    7600 7800 7950 8100 8250 8400 8500];
q_0_w = q_0_w./(3600*24);
x_0 = zeros(1,length(years));
x_1 = zeros(1,length(years));
x_2 = zeros(1,length(years));
x_3 = zeros(1,length(years));
x_4 = zeros(1,length(years));
q_0 = zeros(1,length(years));
q_1 = zeros(1,length(years));
q_2 = zeros(1,length(years));
q_3 = zeros(1,length(years));
q_4 = zeros(1,length(years));
years = 1:1:20;

%% inlet conditions
```

```
for i = 1:length(years)

x_0(i) = (q_0_oil(i))/(q_0_w(i) + q_0_oil(i));
q_0(i) = (q_0_oil(i) + q_0_w(i));
q_oil = 0.0810; %[m^3/s]
q_water = 0.0104; %[m^3/s]

%% gravity separator

[x_1_a, q_1_a] =  gravity_separator(x_0(i), q_0(i)/2);
[x_1_b, q_1_b] =  gravity_separator(x_0(i), q_0(i)/2);
x_1(i) = x_1_a;
q_1(i) = q_1_a + q_1_b;


%% flotation
avg_drop_size = 200;

gas_flow = 0.025; %[m3/s]

[x_2(i), q_2(i), tau1] = flotation_model(x_1(i), q_1(i), avg_drop_size,
    gas_flow);

[x_3(i), q_3(i), tau2] = flotation_model(x_2(i), q_2(i), avg_drop_size,
    gas_flow);

end

years = 2:1:10;
figure()
plot(years, x_0(1:9), '*')
hold on
plot(years, x_1(1:9), '*')
```

```
hold on
plot(years, x_2(1:9), '*')
hold on
plot(years, x_3(1:9), '*')
hold on
plot(years, 0.03*ones(1,length(years)))
legend('x0, inlet from reservoir','x1, outlet gravity separator','x2, outlet first IGF', 'x3, outlet second IGF', '30 ppm')
xlabel('Time [year]')
ylabel('Oil fraction in waster water [-]')
title('Case 3: Oil fractions for year 2 to 10')


figure()
plot(years, q_0(1:9), '*')
hold on
plot(years, q_1(1:9), '*')
hold on
plot(years, q_2(1:9), '*')
hold on
plot(years, q_3(1:9), '*')
legend('q0, inlet flow from reservoir','q1, outlet flow gravity separator', 'q2, outlet flow first IGF', 'q3, outlet flow second IGF', 'Location' ,'southeast')
xlabel('Time [year]')
ylabel('Flow [m3/s]')
title('Case 3: Liquid flows year 2 to 10')
```

F.4 Gravity separator

The following function was used to calculate the outlet fraction and flow from the gravity separator given the inlet fraction and flow.

```

function [x_1, q_1] = gravity_separator(x_0, q_0)
```

```
D = 1.47; % Diameter
L = 7.34;  % length
V_GLS = pi*(D)^2*(1/4)*L; % volume column
k = 0.003; % user specified constants
x_1 = x_0*exp(-k*V_GLS/(q_0)); % function
q_1 = (q_0*(1-x_0))/(1-x_1); % outlet flow
end
```

F.5 Gas flotation

The following function was used to calculate the outlet fraction and flow from the flotation unit given the inlet fraction and flow. The model calculates the

```

function [x_3, q_out, residence_time] = flotation_model(x_in, q_in,
    avg_drop_size, V_flow_gas)

%% fixed constants

C_oil = x_in; % [kg/m3]
x_water = 1-C_oil;
q_oil = q_in*C_oil;
q_water = q_in*x_water;

rho_oil = 870; %[kg/m3]
rho_water = 998; %kg/m3
rho_gas = 1.205;  %kg/m3, utgangspunkt
dyn_vis = 8.9*10^-4; %kg/m*s T = 10C, dynamic viscoity water
g = 9.81; %m/s2
R_oil = (1/2)*avg_drop_size*10^-6; %[m] = 150 microns
R_gas = 400*10^-6; % [m], 400 microns

%% Volume
H = 2; %2.5m
r = 0.5;
```

```
A = pi*r^2;
V = A*H; %volume tank

%% velocities - gas and oil in tank. - stokes law

vel_oil = q_in/A; % [m/s]
vel_gas = (2/9)*(rho_water-rho_gas)/(dyn_vis) *g*R_oil^2; % [m/s]
rel_vel = (vel_gas+vel_oil); %[m/s]

%% residence time oil

residence_time = H/vel_oil; % [sek]

%% bubbles oil
V_oil_total = C_oil*V/(rho_oil); % [m3] total oil in tank
V_oil_particle = (4/3)*pi*R_oil^3; % [m3] - volume bubble
bubbles_oil_init = V_oil_total/V_oil_particle; % [#bubbles oil]
bubbles_oil_cons = bubbles_oil_init/V;  %[bubbles oil/m3]

%% bubbles gas
V_gas_bubble = (4/3)*pi*R_gas^3; % [m3] gas bubble volume
bubbles_gas_tot = V_flow_gas*residence_time/V_gas_bubble;%[#bubbles gas]
bubbles_gas = bubbles_gas_tot/V; %[bubbles gas/m3]

%% bubble-capture efficency

E = 1/1000; % amount of collisions that lead to capture

%% calculations - bubble collisions

dt = 1;
t_max = residence_time;
t = 1:1:t_max;
bubbles_oil = zeros(0,length(t));
bubbles_oil(1) = bubbles_oil_cons;
```

```
for i = 1:length(t)-1
    Z = (1/2)*E*bubbles_oil(i)*bubbles_gas*pi*(R_gas+R_oil)^2*rel_vel*dt;
    bubbles_oil(i+1) = bubbles_oil(i)-Z;
end

%% plot - change in ppm

ppm_oil = zeros(0,length(t));
for i = 1:length(t)
    ppm_oil(i) = 10^3*(bubbles_oil(i)*V_oil_particle)*rho_oil;
end

FINAL_CONCENTRATION = min(ppm_oil);

%% plot - concentration profile in tank - not presented in report

%H_min = H;
%H_vec = H_min-H_min/t_max:-H_min/t_max:0;
%plot(H_vec, ppm_oil,'red')
%set ( gca, 'xdir','reverse')
%title('Concentration profile')
%xlabel('Height tank')
%ylabel('ppm oil')

x_3 = FINAL_CONCENTRATION/1000; % convert from ppm to fraction

q_out = (q_in*(1-x_in))/(1-x_3); % calculate outlet flow

end
```

F.6 Hydrocyclone

The following function was used to calculate the outlet fraction and flow from the hydrocyclone given the inlet fraction and flow.

```matlab


function [x_out, q_out, avg_size, num_liners_min, num_liners_max, sep_eff] = hydrocyclone(q_in, x_in, R_hyd) % q_in[m3/s]
%% separation efficency as a function of particle diameter
D = 0.075; % 7.5cm, body diameter
[Di, len] = sizing(D); % inlet diameter and length of hydrocyclone.
N_hy = HCN(Di, q_in, x_in); % hydrocyclone number

rho_oil = 870; % [kg/m3]
rho_water = 998; %[kg/m3]
dyn_vis = 8.9*10^-4; % [kg/m*s] at T = 10C, dynamic viscoity water

d_75 = sqrt(N_hy*dyn_vis*D^3/(q_in*(rho_water-rho_oil)));
r_75 = d_75*10^6/2; %the distribution is in radius.

r = 1:1:R_hyd;
sep_eff = zeros(1,length(r));
%emperical constants
c3 = -1.2; %[-]
c4 = 0.35; %[-]
c5 = 0.3; %[-]
%obs: bruker her r_75 for  v re konsistent, men gir samme svar.
for i = 1:length(r)
    sep_eff(i) = 1 - exp(c3*(r(i)/r_75-c4)^(c5)); % calculating efficiency as a function of radius
end

sep_eff(sep_eff~=real(sep_eff)) = 0;

plot(r, sep_eff)
xlabel('oil radius [mikro-m]')
ylabel('separation efficency[-]')
hold on

```

```
[y, sizes] = distribution(R_hyd, x_in); % inlet distribution


hydrocyclone_dist = zeros(1,length(sizes));
avg_size = 0;
for i = 1:length(sep_eff)
    hydrocyclone_dist(i) = y(i)*(1-sep_eff(i)); %outlet distribution
    avg_size = avg_size + sizes(i)*hydrocyclone_dist(i); %sum of all the sizes
end

%plot the inlet and outlet distribution
bar(sizes,y, 0.3)
xlabel('size [mikro-m]')
ylabel('fraction')
hold on
bar(sizes, hydrocyclone_dist)
xlabel('size [mikro-m]')
ylabel('fraction')

x_out = sum(hydrocyclone_dist); % fraction out is the sum of all the fractions ..
% for all oil droplet sizes.

q_out = (q_in*(1-x_in))/(1-x_out); % caluclating outlet flow.

avg_size = avg_size/x_out; % calculating the average sizes, used in flotation function

[num_liners_min, num_liners_max] = liners(q_in);

end

function [num_liners_min, num_liners_max] = liners(q_in)
    q_max = 9; %[m3/h] from graph
```

```
    q_min = 2.1; %[m3/h] from graph
    q_in = q_in *3600;  % [m3/h]
    num_liners_min = q_in/q_max;
    num_liners_max = q_in/q_min;
end

function hydrocyclone_number = HCN(Di, q_in, x_in) % D is here inlet
    diameter
rho_oil = 870;
rho_water = 998;
rho = rho_oil*x_in + rho_water*(1-x_in);
dyn_vis = 0.001139;
[num_liners_min, num_liners_max] = liners(q_in);
avg_liners = (num_liners_min + num_liners_max)/2; % use the average number
    of liners
q_in = q_in/avg_liners; %average flow in each liner

Inlet_Re = rho*q_in*Di/(dyn_vis);
hydrocyclone_number = -7.1428*10^-9*Inlet_Re + 0.0027142; %regression for
    figure 19.

end

function [D_inlet, len] = sizing(D) % diameter upper section
    D_inlet = 0.28*D; % inlet diameter
    len = 5*D;  %length
end
```

F.7 Hydrocyclone in series

The following function was used to calculate the outlet fraction and flow from the hydrocyclones in series given the inlet fraction and flow.

```


```

```
function [x_1, q_1, x_2, q_2] =  hydrocyclone_series(x_in, q_in) % q_in[m3/s]
%% separation efficency as a function of particle diameter
D = 0.075; % 7.5cm, body diameter
R_hyd = 150; % max droplet size
[Di, len] = sizing(D);  % inlet diameter and length of hydrocyclone.
N_hy = HCN(Di, q_in, x_in); % hydrocyclone number

rho_oil = 870; % [kg/m3]
rho_water = 998; % [kg/m3]
dyn_vis = 8.9*10^-4; % [kg/m*s] at T = 10C, dynamic viscoity water

d_75 = sqrt(N_hy*dyn_vis*D^3/(q_in*(rho_water-rho_oil)));
r_75 = d_75*10^6/2; %the distribution is in radius.

r = 1:1:R_hyd;
sep_eff = zeros(1,length(r));
%emperical constants
c3 = -1.2; %[-]
c4 = 0.35; %[-]
c5 = 0.3; %[-]

for i = 1:length(r)
    sep_eff(i) = 1 - exp(c3*(r(i)/r_75-c4)^(c5));
end

sep_eff(sep_eff~=real(sep_eff)) = 0;

%figure()
%plot(r, sep_eff)
%xlabel('oil radius [mikro-m]')
%ylabel('separation efficency[-]')

[y, sizes] = distribution(R_hyd, x_in);

```

```
hydrocyclone_dist_1 = zeros(1,length(sizes));
avg_size = 0;
for i = 1:length(sep_eff)
    hydrocyclone_dist_1(i) = y(i)*(1-sep_eff(i));
    avg_size = avg_size + sizes(i)*hydrocyclone_dist_1(i);
end

hydrocyclone_dist_2 = zeros(1,length(sizes));
avg_size = 0;
for i = 1:length(sep_eff)
    hydrocyclone_dist_2(i) = hydrocyclone_dist_1(i)*(1-sep_eff(i));
    avg_size = avg_size + sizes(i)*hydrocyclone_dist_2(i);
end

%figure()
%plot(sizes,y)
%xlabel('size [mikro-m]')
%ylabel('fraction')
%hold on
%plot(sizes, hydrocyclone_dist_1)
%xlabel('size [mikro-m]')
%ylabel('fraction')
%hold on
%plot(sizes, hydrocyclone_dist_2)
%xlabel('size [mikro-m]')
%ylabel('fraction')

x_1 = sum(hydrocyclone_dist_1);

q_1 = (q_in*(1-x_in))/(1-x_1);

x_2 = sum(hydrocyclone_dist_2);

q_2 = (q_1*(1-x_1))/(1-x_2);

```

```
end

function [num_liners_min, num_liners_max] = liners(q_in)
    q_max = 9; %[m3/h]
    q_min = 2.1; %[m3/h]
    q_in = q_in *3600;% [m3/h]
    num_liners_min = q_in/q_max;
    num_liners_max = q_in/q_min;
end

function hydrocyclone_number = HCN(Di, q_in, x_in)
rho_oil = 850;
rho_water = 998;
rho = rho_oil*x_in + rho_water*(1-x_in);
dyn_vis = 0.001139;
[num_liners_min, num_liners_max] = liners(q_in);
avg_liners = (num_liners_min + num_liners_max)/2;
q_in = q_in/avg_liners; %gjennomsnittlig str m i hver liner

Inlet_Re = rho*q_in*Di/(dyn_vis);
hydrocyclone_number = -7.1428*10^-9*Inlet_Re + 0.0027142;

end

function [D_inlet, len] = sizing(D) % diameter upper section
    D_inlet = 0.28*D;
    len = 5*D;
end
```

F.8 Sizing gravity separator

The following function was used to calculate the dimensions of the gravity separator.

```


```

```
function [V, Lv, Dv, Act_res] = sizing_column(q_liq , q_vap)
%% egendefinert
rho_liq = 950;%sjekk [kg/m3]
rho_vap = 0.67; %sjekk [kg/m3]
m_liq = rho_liq*q_liq*3600*(1/2); %mass flow liquid [kg/h]
m_vap = rho_vap*q_vap*3600*(1/2); %mass flow vap [kg/h]
fv = 0.8; %fraction vapour in column
ld_factor = 5; %p>35bar
hv = 0.5; %Dv/2

%% utregning
u_s= 0.15*0.07*sqrt((rho_liq-rho_vap)/rho_vap); %no demister pad
Vap_vol_flow = m_vap/(3600*rho_vap); %[m3/s]
cross_A_factor = pi/4*fv;
u_v = Vap_vol_flow/cross_A_factor; %*Dv^-2
settle_factor = hv/u_s; %*Dv
Act_res = ld_factor/(u_v); %*Dv^3

Dv = sqrt(settle_factor/Act_res);
Lv = ld_factor*Dv
V = Lv*Dv^2*pi/4;

req_res = 3; %requires residence time = 3min
hold_up_time = 3; %initializing while loop
liq_vol_flow = m_liq/(3600*rho_liq);

while req_res >= hold_up_time
Dv = Dv*(req_res/hold_up_time)^fv;
Lv = ld_factor*Dv;
liq_cross_A = pi*Dv^2/4*fv;
hold_up_V = liq_cross_A*Lv;
hold_up_time = hold_up_V/liq_vol_flow*(1/60); %[min]
end
end
```

F.9 Distribution

The following function was used to calculate the bubble distribution after the hydrocyclone.

```

function [y, sizes] = distribution(A, x_0)

sizes = zeros(1,A);
for i = 1:length(sizes)
    sizes(i) = i;
end

mu = sum(sizes)/length(sizes);
sigma = 30;
y = normpdf(sizes, mu, sigma);
y = y*x_0; % slik at summen av y skal v re lik molfraksjonen
end
```

F.10 NPV calculation

The following script was used to calculate the NPV.

```

function NPV = return_NPV(CAPEX, OPEX, oil_price)
q_oil = [5565 5970 7000 6900 6700 6500 6100 5600 5000 4200].*333.33;%[m3/year]
q_gas = q_oil.*100; %[m3/d] GOR = 100;
years = 1:1:10;
bbl = 6.289814; % 1m3 = 6.289814 bbl;
MMBtu = 1/28.263682;
q_oil = q_oil.*bbl;
q_gas = q_gas.*MMBtu;
gas_price = 4.272; % USD/MMBtu
NI = zeros(1,length(years));
tax_rate = 0.78; %78
for i = 1:length(years)
    NI(i) = (q_oil(i)*oil_price + q_gas(i)*gas_price - OPEX)*(1-tax_rate);
```

```
end

r = 0.1; %0.1504

yearly_NPV = zeros(1,length(years)+1);
yearly_NPV(1) = -CAPEX;
for i = 1:length(years)
    yearly_NPV(i+1) = yearly_NPV(i) + NI(i)/(1+r)^(i);
end

years_2 = 0:1:10;
ar = area(years_2, yearly_NPV./10^6, 'FaceColor', 'flat')
ec = ar.FaceColor;
ar.FaceColor = [0 0.75 0.75];
xlabel('Time [years]')
ylabel('Discounted After Tax Cash Flow [mill. USD]')
title('Cash Flow Diagram')

NPV = yearly_NPV(end);
end
```

F.11 Sensitivity analysis

The following scrip was used to create the sensitivity analysis.

```
%% Fixed oil price, OPEX, CAPEX
oil_price = 67; % USD/bbl;
OPEX = 27220968;
CAPEX = 485669379;
NPV = return_NPV(CAPEX, OPEX, oil_price);

%% Sensitivity analysis
variable_change = 60;
var = zeros(1, variable_change*2+1);
oil_pm = zeros(1, variable_change*2+1);
```

```
CAPEX_pm = zeros(1, variable_change*2+1);
OPEX_pm = zeros(1, variable_change*2+1);


NPV_OPEX = zeros(1, variable_change*2+1);
NPV_CAPEX = zeros(1, variable_change*2+1);
NPV_oil_price = zeros(1, variable_change*2+1);

for i = 1:length(var)
    if i < variable_change
        var(i) = i-variable_change -1;

    elseif i > variable_change
        var(i) = i-variable_change -1;
    end
        CAPEX_pm(i) = CAPEX*(1+var(i)/100);
        NPV_CAPEX(i) = return_NPV(CAPEX_pm(i), OPEX, oil_price);

        OPEX_pm(i) = OPEX*(1+var(i)/100);
        NPV_OPEX(i) = return_NPV(CAPEX, OPEX_pm(i), oil_price);

        oil_pm(i) = oil_price*(1+var(i)/100);
        NPV_oil_price(i) = return_NPV(CAPEX, OPEX, oil_pm(i));
end

plot(var, NPV_CAPEX./10^6)
hold on
plot(var, NPV_OPEX./10^6)
hold on
plot(var, NPV_oil_price./10^6)
hold on
plot(var, ones(1,length(var))*NPV_CAPEX(variable_change)/10^6,'.')
xlabel('Change in parameter [%]')
ylabel('NPV [mill usd]')
legend('CAPEX','OPEX', 'Oil Price', 'Base case', 'location', 'southeast')
```

```
title('Sensitivity analysis')
```

F.12 Profitability measurements

The following script was used to calculate IRR, ROI, and payback time.

```

q_oil = [5565 5970 7000 6900 6700 6500 6100 5600 5000 4300].*333.33;%[m3/year]
q_gas = q_oil.*100; %[m3/d] GOR = 100;
oil_price = 67; % USD/bbl;
OPEX = 27220968;
CAPEX = 485669379;
years = 1:1:10;
bbl = 6.289814; % 1m3 = 6.289814 bbl;
MMBtu = 1/28.263682;
q_oil = q_oil.*bbl;
q_gas = q_gas.*MMBtu;
gas_price = 4.272; % USD/MMBtu
CF = zeros(1,length(years));
tax_rate = 0.78; %25
for i = 1:length(years)
    CF(i) = (q_oil(i)*oil_price + q_gas(i)*gas_price - OPEX)*(1-tax_rate);
end

IRR = irr([-CAPEX, CF]);

avg_CF = sum(CF)/length(CF);

ROI = avg_CF/CAPEX;

tPB = CAPEX/avg_CF;
```